

A New DA and TM Based Approach to Design Air-Core Magnets

Shashikant Manikonda

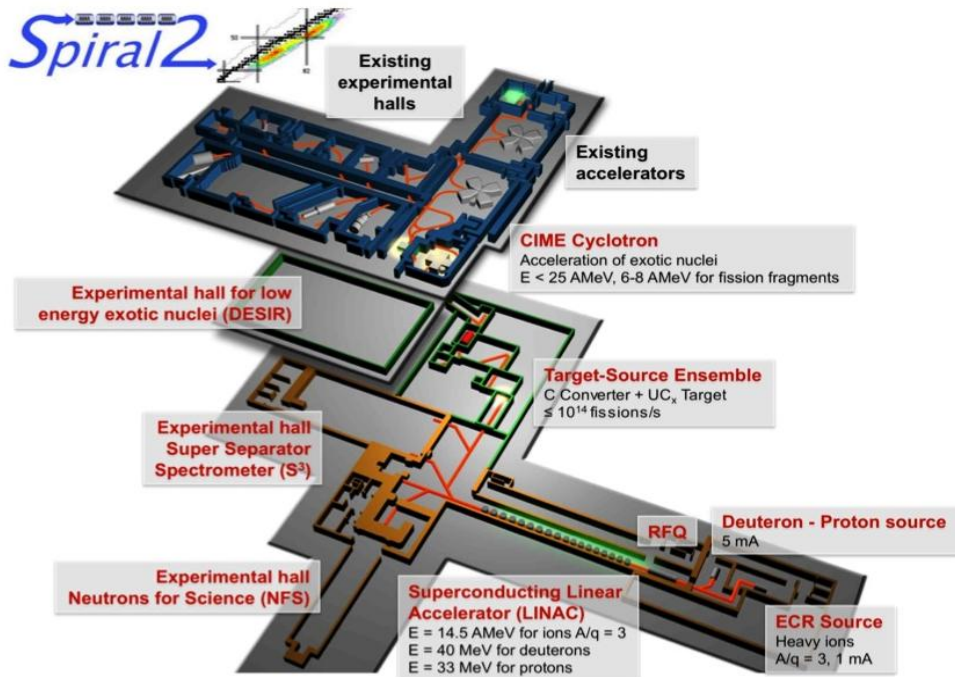
*Taylor Model Methods VII,
Dec 14th-17th, 2011, Key West, Florida*

S3 device at SPIRAL2

- SPIRAL2 is a project to expand the capabilities of the GANIL, France facility in nuclear physics research with exotic beams
- One of the new instruments is the **Super Separator Spectrometer (S³)** for high intensity stable heavy ion beams.

Technical challenges for S³:

- Separation of very rare events from intense backgrounds
- Large beam acceptance and high selectivity for weak reaction channels are required



Interesting Experiments

The ¹⁰⁰Sn factory

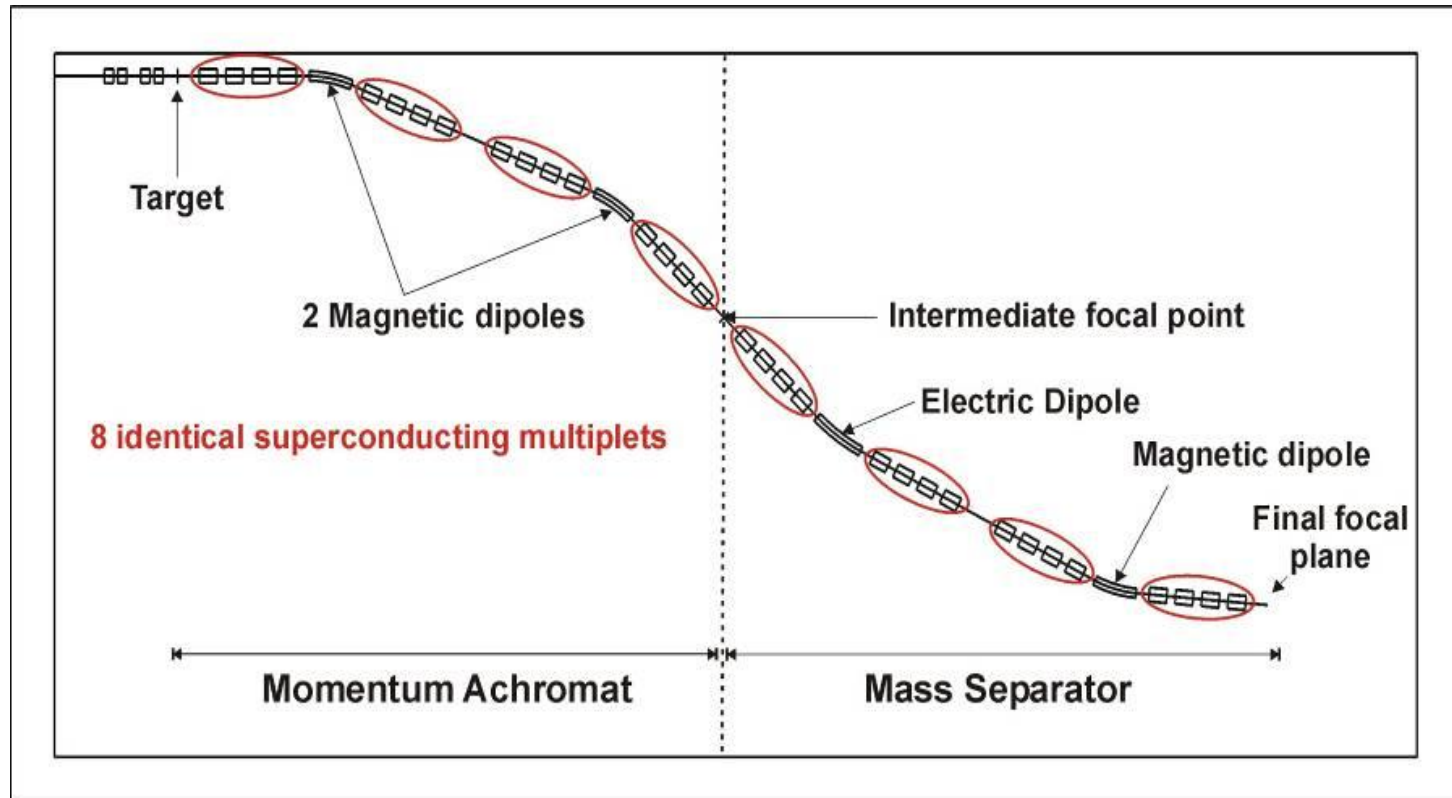
| | |
|--|--|
| $N = Z$ $^{58}\text{Ni} + ^{46}\text{Ti} \rightarrow$ $^{100}\text{Sn} + 4n$ | Ground state properties (half-lives, masses, spectroscopy) |
| | |

SHE / VHE - Fusion-evaporation in direct kinematics

| | |
|---|--|
| SHE / VHE $^{48}\text{Ca} + ^{248}\text{Cm} \rightarrow$ $^{292}\text{116} + 4n$ | Synthesis and delayed spectroscopy |
| | Chemistry |
| | Ground state properties (half-lives, masses, spectroscopy) |

MAMS Layout for S^3

- 36m x 16m room layout
- Baseline MAMS configuration uses 8 quadruplets of multipoles with quadrupole, sextupole, & octupole coils



Momentum Achromat followed by Mass Separator design (MAMS)

S3 Device Description

- ❑ Excellent primary beam suppression (10^{13}) at 0°
- ❑ Total transmission better than 50% for the two selected experiments
 - ❑ $^{48}\text{Ca} + ^{248}\text{Cm} \rightarrow ^{292}116 + 4n$
 - ❑ $^{58}\text{Ni} + ^{48}\text{Ti} \rightarrow ^{100}\text{Sn} + 4n$
 - ❑ *This corresponds to:*
 - ❑ *charge state acceptance of $\pm 10\%$, 5 charge states with $\langle Q \rangle = +20$*
 - ❑ *momentum acceptance for each charge state of $\pm 10\%$*
 - ❑ *large angular acceptance in both planes of ± 50 mrad*
- ❑ Maximum magnetic rigidity $Br_{\text{max}} = 1.8 \text{ Tm}$ (*momentum achromat*)
- ❑ Maximum electric rigidity $Er_{\text{max}} = 12 \text{ MV}$
- ❑ Resolving power > 300 (FWHM) for physical separation in m/q
- ❑ Beam spot on the production target of S^3 of either:
 - ❑ $\sigma_x = 0.5 \text{ mm (Gaussian)} \times \sigma_y = 2.5 \text{ mm (Gaussian)}$ or
 - ❑ $\sigma_x = 0.5 \text{ mm (Gaussian)} \times \Delta y = 10 \text{ mm (uniform)}$

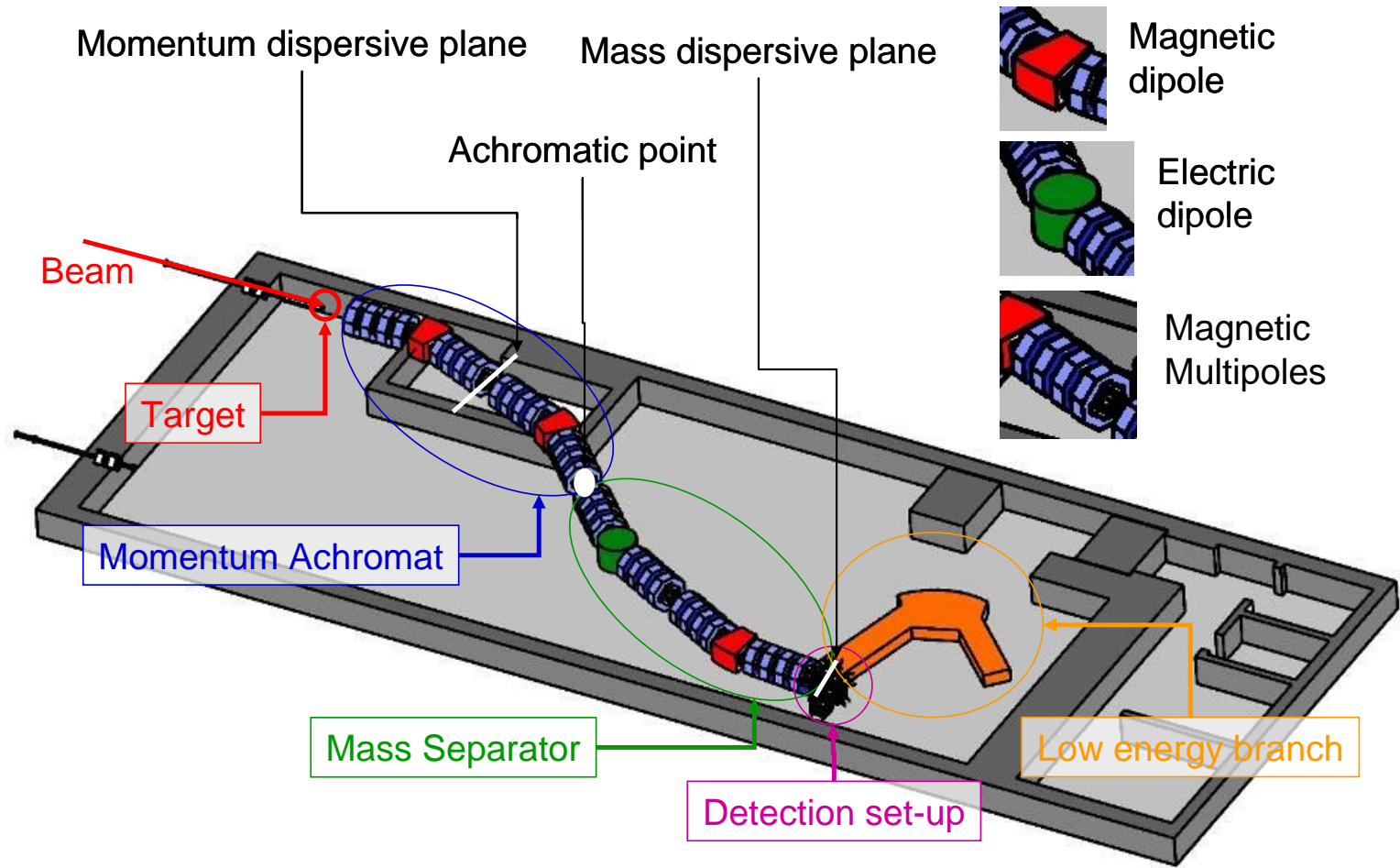


S3 Device Description (Continued)

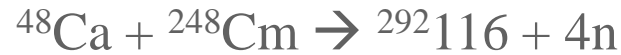
- ❑ Final focal plane size depending on the experiment
 - ❑ *200 x 100 mm (maximum for high resolution mode, e.g. SHE synthesis)*
 - ❑ *100 x 100 mm (delayed gamma spectroscopy)*
 - ❑ *50 x 50 mm (low-energy branch gas catcher, GS properties)*
- ❑ Mass Achromat followed by Mass Separator (MAMS) layout chosen for S³
 - ❑ Momentum achromat to suppress primary beam by at least 1:1000.
 - ❑ Further beam suppression and mass channel selection by a mass separator stage which is fully achromatic in momentum for each m/q value.
- ❑ Different operating modes are envisioned for performing experiments



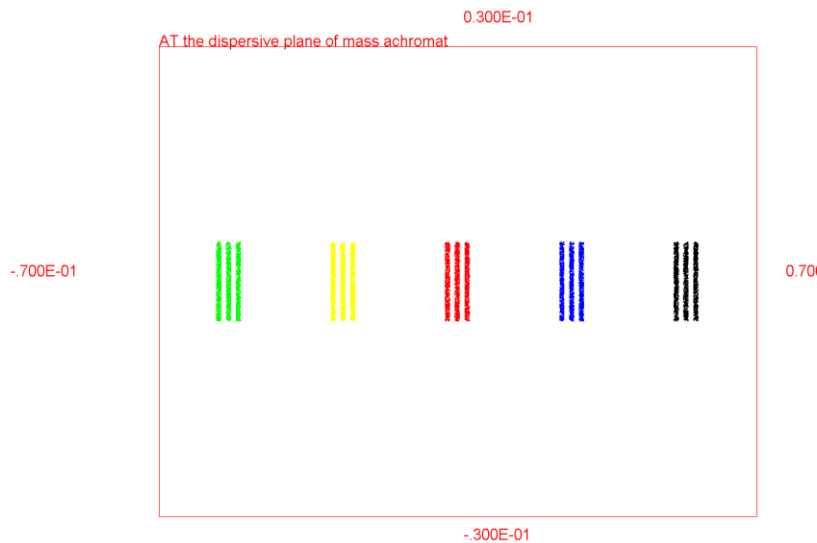
Layout in S3 room



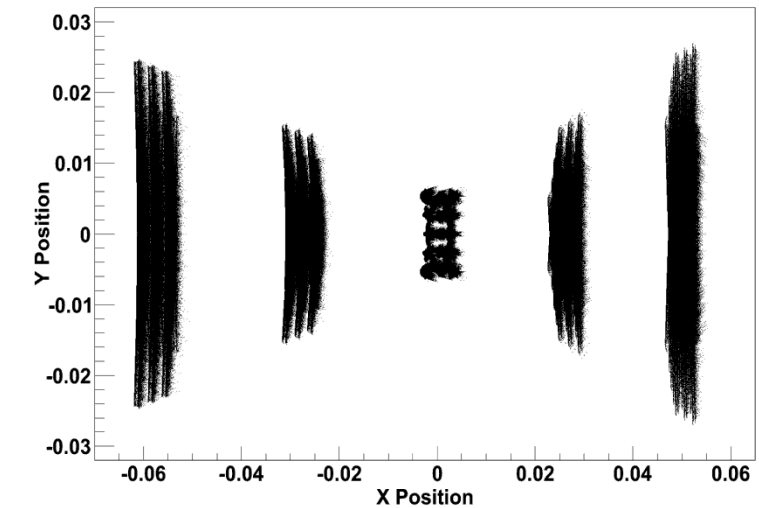
X-Y plot at the mass focal plane: SHE



5 charge states selected by slits into
a 7-cm x 3-cm catcher or detector



First Order



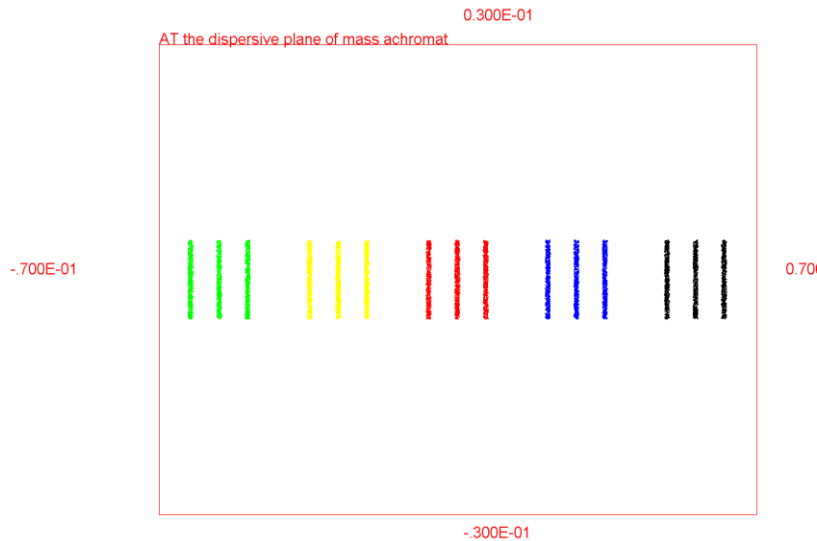
Second Order

Mass-energy aberrations corrected

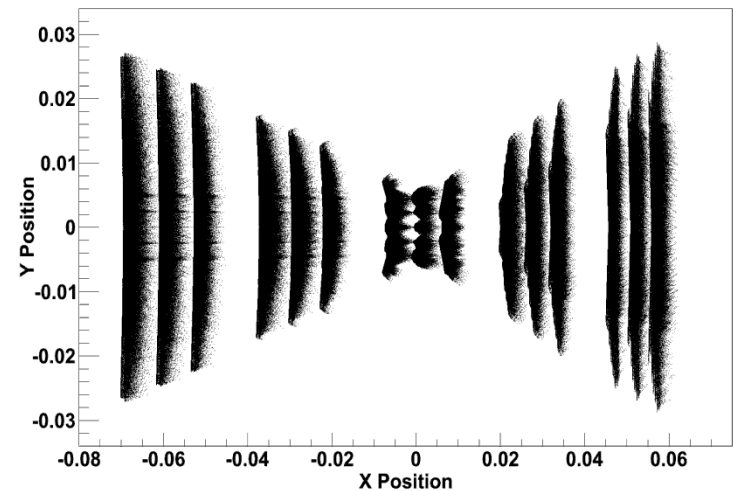
X-Y plot at the mass focal plane: NEZ



5 charge states selected by slits into
a 7-cm x 3-cm catcher or detector



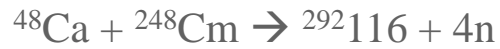
First Order



Second Order

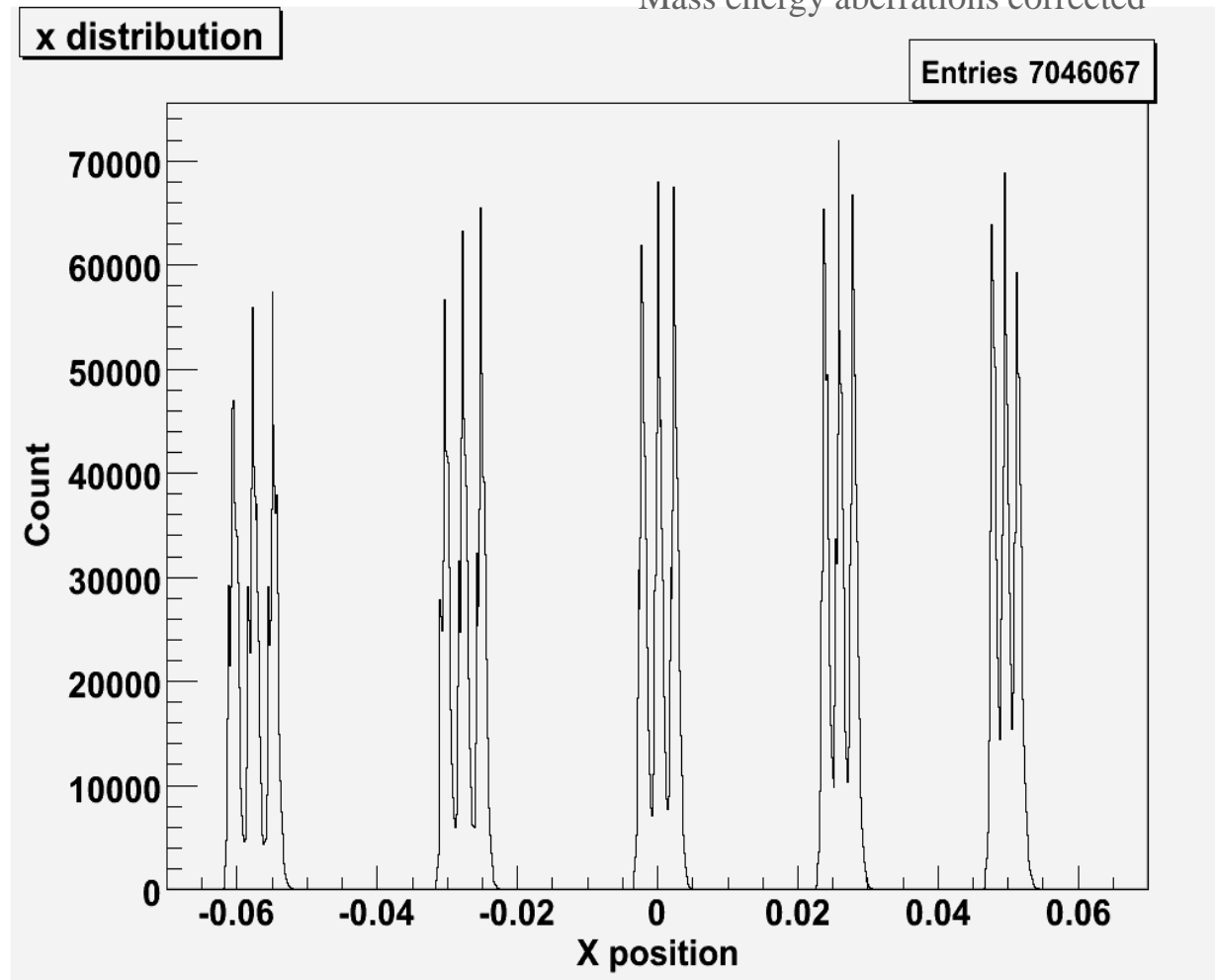
Mass-energy aberrations corrected

Histogram at mass focal Plane



$$\delta Q = \pm 2, \delta m = \pm 1, \Delta B\rho = 4.6\%$$

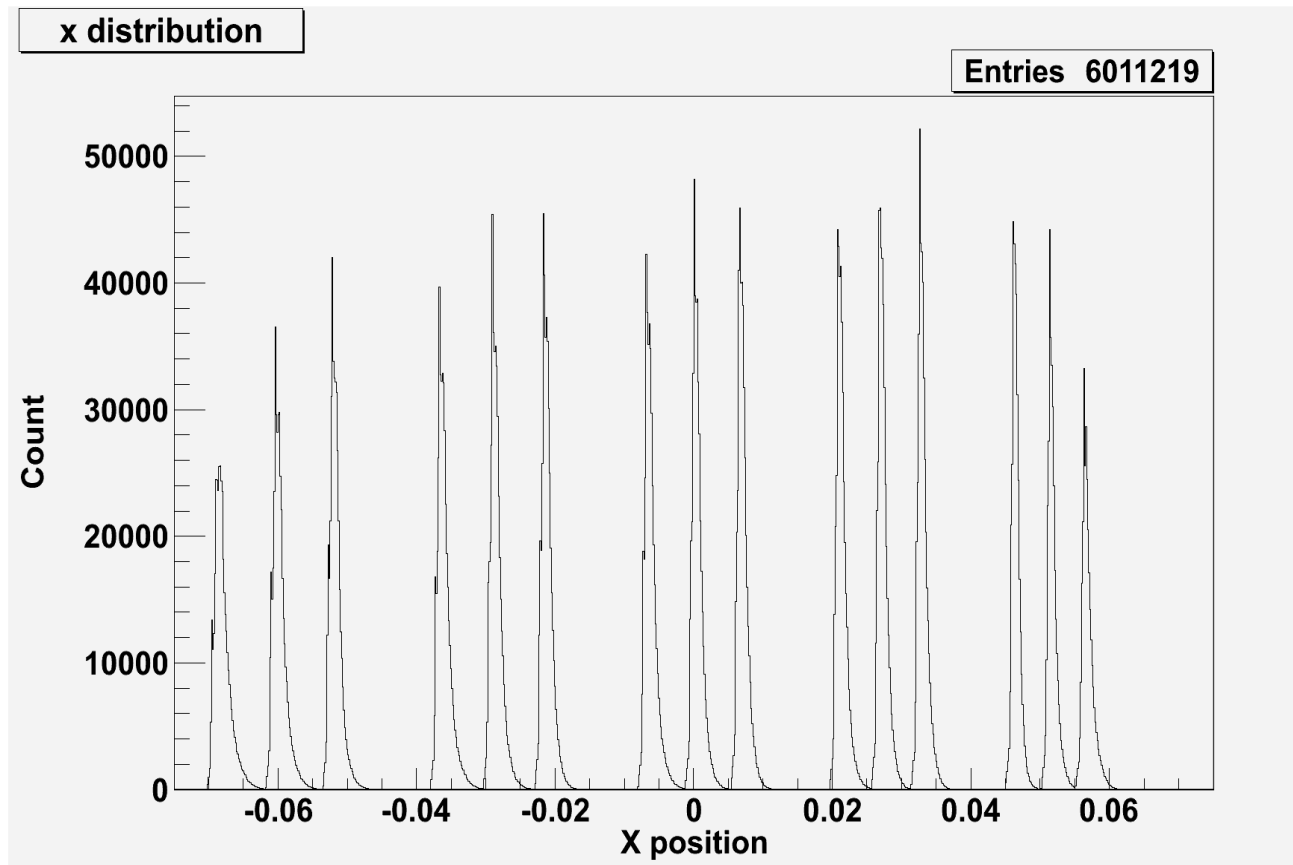
Mass energy aberrations corrected



Plot showing position of mass line



$\delta Q = \pm 2$, $\delta m = \pm 1$, $\Delta B\rho = \pm 7.5\%$



Plot showing position of mass line

Magnet requirements for S3

- 8 SC quadruplets or triplets
- 3 dipoles and 1 electrostatic sector magnet
- Each singlet has quadrupole, sextupole, & octupole coils, with 30-cm warm bore diameter & 40-cm effective length (octupoles may not be required)
- Fields required at 15-cm radius for 2 T-m rigidity (higher rigidity is easy):
 - Quadrupole: 1.0 T
 - Sextupole: 0.3 T
 - Octupole: 0.3 T
- Total power required for cryo-coolers of 8 quadruplets ~160 kW
 - Warm iron used to speed up cool down (~1 ton per multipole)
- Options for Multipole Magnet Design
 - Race track Coils
 - Double Helix Model by AML
 - 3D Cosine theta magnets



Type of Magnets

The electric and magnetic field will depend on the type of magnets we choose.

Some examples:

- Bending magnets (Dipole)
- Focusing magnets (Quadrupole)
- Steering magnets
- Kicker magnets (thin Quadrupole)
- Accelerating (Electric element)
- Corrector magnets (Hexapole, Octupole etc)

Accelerator lattice consists of array of magnets setup to attain certain goal. Complexity comes from the fact that there are **many** undetermined parameters. To arrive at a final (fully optimized) beam optic layout requires **several** iterations between beam optic design studies, magnet design studies and other practical constraints.

Magnets for Accelerator Physics Applications

Some factors influencing the choice of magnets and the design of magnets

- Bp and Ep of the beam/recoil
 - High Energy Physics: Only magnetic elements can be used
 - Low Energy Nuclear Physics (<10 MeV/nucleon): Both Electric and Magnetic elements can be used
- Field quality requirement
- Operating environment: Radiation Hardened magnets
- Super conducting or conventional: Depends on field strength requirements
- Tolerances to errors, misalignments, stress and strain in the support structures, heating
- Practical constraints like positioning of beam dumps, detectors, slits, monitors etc.
- Other factors: Reuse of existing magnets

- During the design phase:
 - Is the magnet practically feasible to build ?
 - Field quality requirement
 - Cost estimate
 - Beam optic properties (Transfer Maps)
 - Fringe Fields
 - Misalignment study
- After construction
 - Transfer maps with realistic fields



Some magnet Modelling codes/tools

- TOSCA module OPERA package
 - 3D code, uses Finite Element Method (FEM)
- ROXIE code from CERN
 - 3D code, uses many modes including hybrid Boundary Element Method & Finite Element Method
- POISSON
 - 2D Magnetostatic code, uses FEM
- SIMON
 - 3D code, uses Finite Difference method (FDM)
- RADIA (Free)
 - 3D Magnetostatic code, uses Boundary Element Method (BEM)

Pre-processor → Field Solver → Post-processor

Magnetic field due to arbitrary current distribution

- Magnetic field due to arbitrary current distribution is computed using the Biot-Savart law or Ampere's law

$$\vec{B}(\vec{r}) = \int \frac{1}{4\pi\mu_0} \frac{\vec{I} \times \vec{dl}}{|\vec{r} - \vec{r}_s|^2}$$

- Implementation:
 - Discretize the domain into current elements
 - DA framework is developed to describe a current element for the line, surface and volume case
 - Expand the kernel for the Biot-Savart law or Ampere's law
 - Integrate with respect to the variables describing the current elements
 - Sum over all the current elements
- The curl and the divergences for the field computed is always zero in the current free region.
- Number of current elements required is less due to use of High order
- Now the magnet design, beam optics and optimization can be done in the same code



Taylor model Integration

Let (P_n, I_n) be an n -th order Taylor model of f . From this we can obtain a Taylor model for the indefinite integral $\partial_i^{-1} f = \int f dx'_i$ with respect to variable x_i .

Taylor polynomial part: $\int_0^{x_i} P_{n-1} dx'_i$,

Remainder Bound: $(B(P_n - P_{n-1}) + I_n) \cdot B(x_i)$, where $B(P)$ is a polynomial bound.

So define the operator ∂_i^{-1} on space of Taylor models as

$$\begin{aligned} & \partial_i^{-1}(P_n, I_n) \\ &= \left(\int_0^{x_i} P_{n-1} dx'_i, (B(P_n - P_{n-1}) + I_n) \cdot B(x_i) \right) \end{aligned}$$

$$\int_{x_{il}}^{x_{iu}} f(\vec{x}) dx_i \in \left(P_{n, \partial^{-1} f}(\vec{x}|_{x_i=x_{iu}-x_{i0}}) - P_{n, \partial^{-1} f}(\vec{x}|_{x_i=x_{il}-x_{i0}}), I_{n, \partial^{-1} f} \right)$$

This method has following advantages:

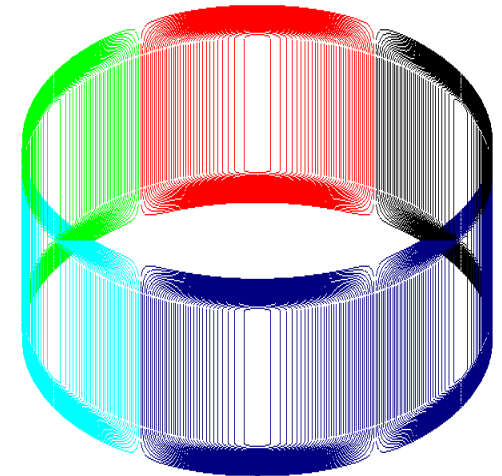
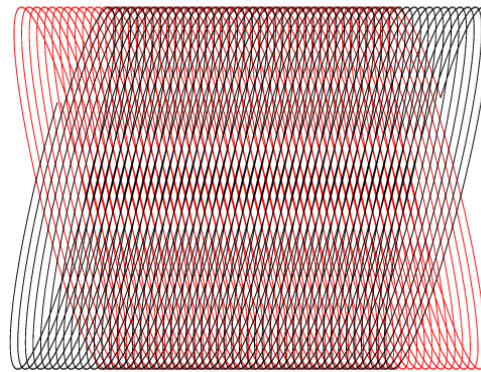
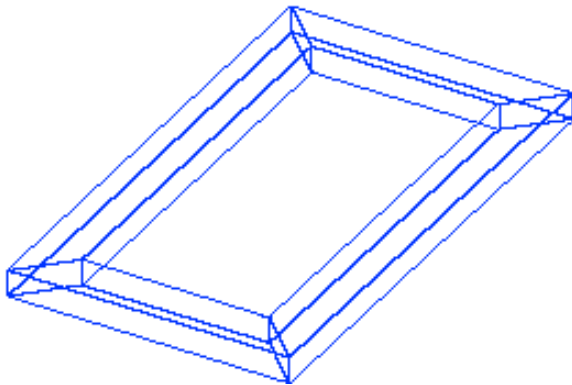
- No need to derive quadrature formulas with weights, support points x_i and an explicit error formula
- High order can be employed directly by just increasing the order of the Taylor model, limited only by the computational resources
- Rather large dimensions are amenable by just increasing the dimensionality of the Taylor models, limited only by computational resources



Tools

Due to their frequent use in the accelerator magnet applications, a dedicated set of tools has been written in the code COSY INFINITY for

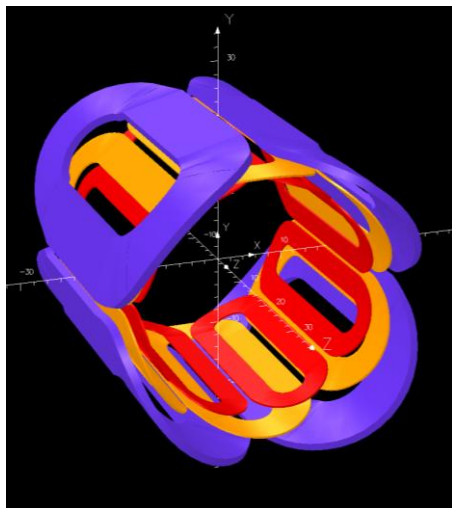
- Infinitely long rectangular cross section current wire(2D design)
- Finite length rectangular cross section current wire
 - Current coil of rectangular cross section (3D design)
- Double Helix Model
- Cosine-theta type Magnet model



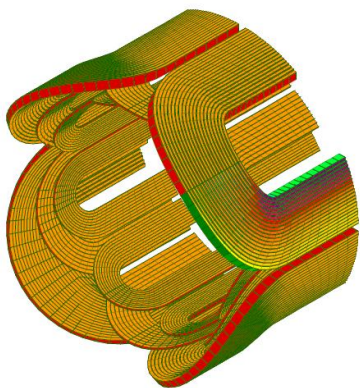
In addition to extracting the transfer maps these tools can be used to do conceptual design of magnets



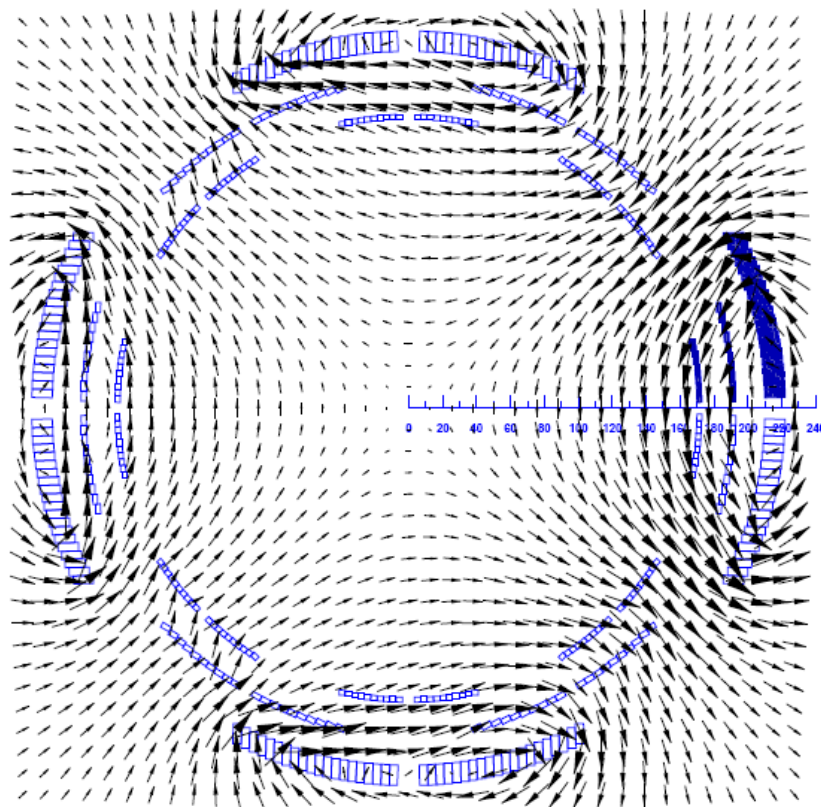
S3 Multipole magnet : using racetrack coils



3D coil configuration model using OPERA3D Code



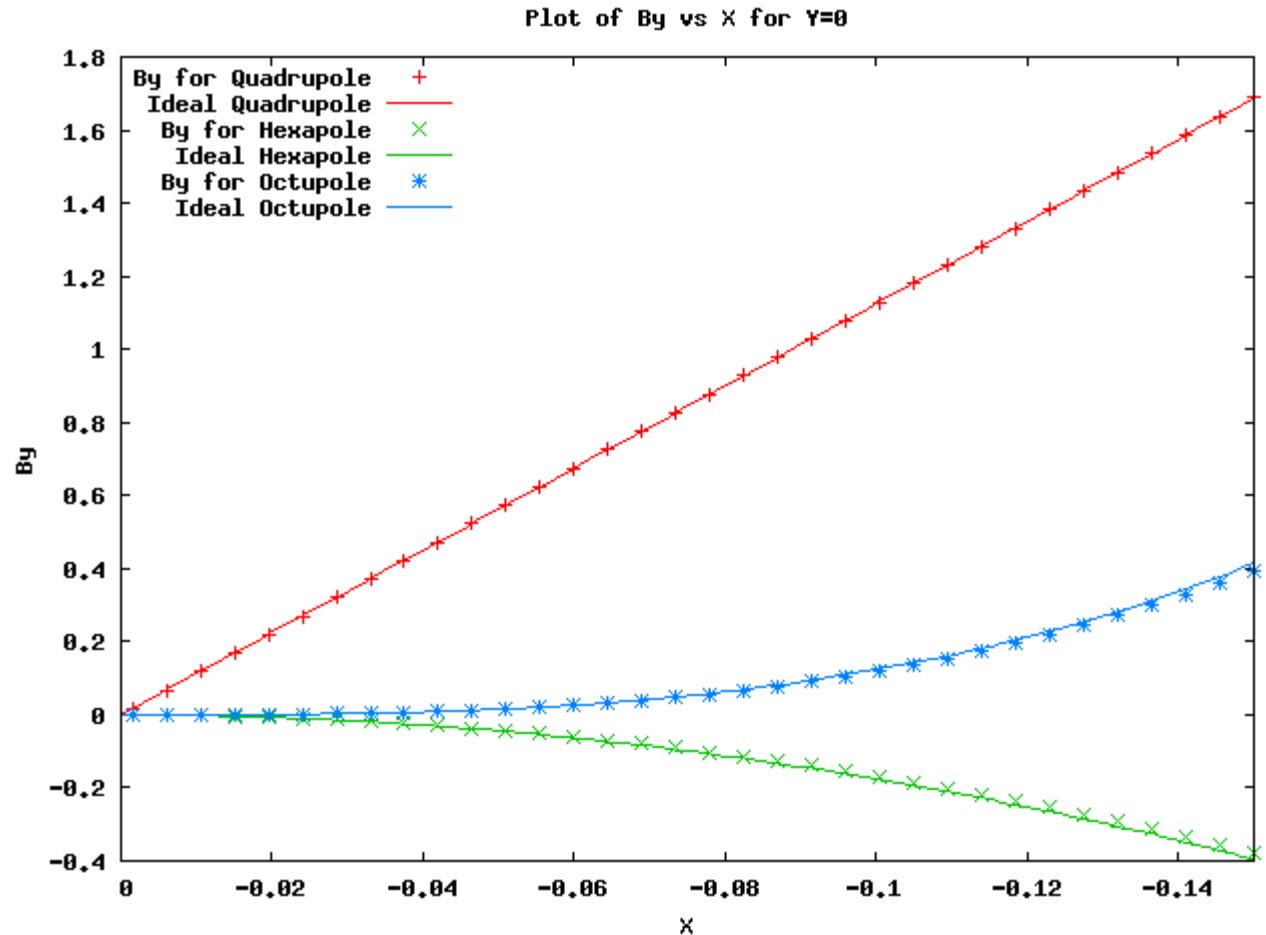
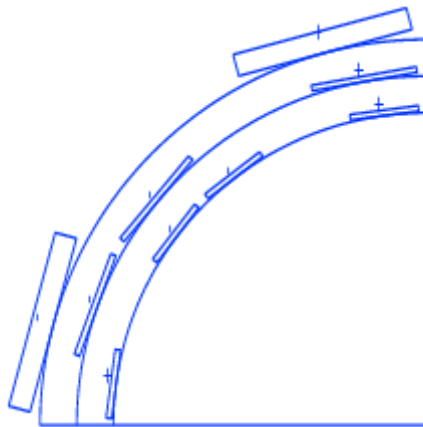
3D coil configuration model using ROXIE Code



Cross section layout and vector plot of the field



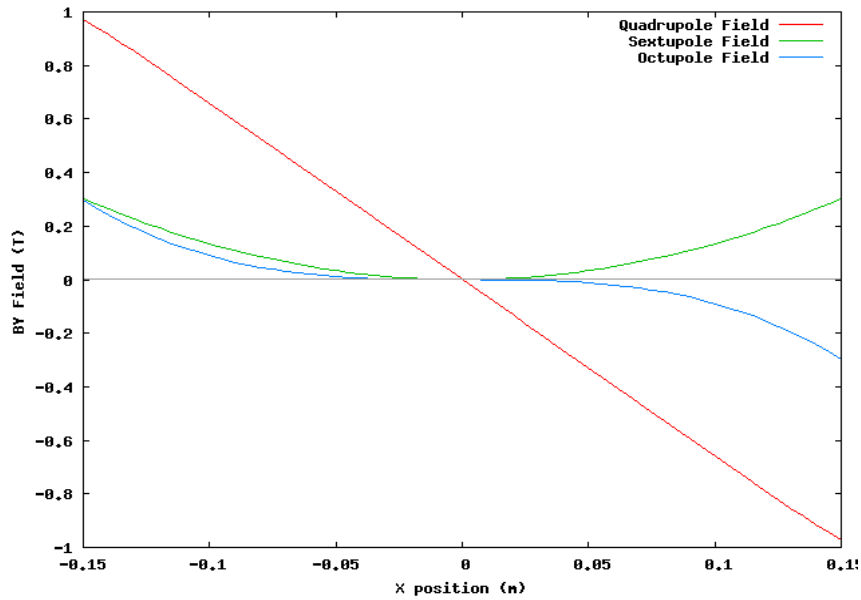
S3 Multipole magnet : using racetrack coils



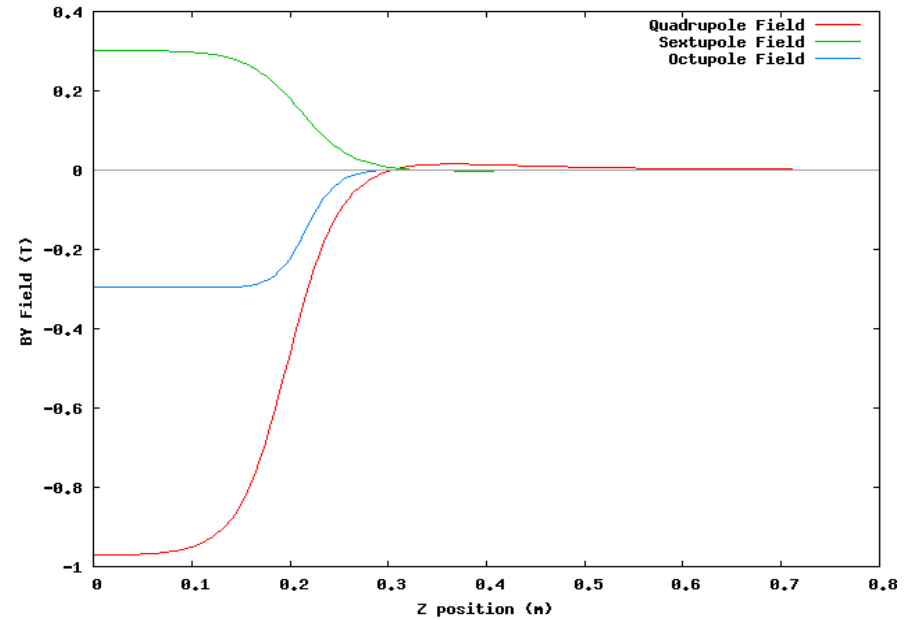
“Manikonda, S.; Nolen, J.; Berz, M. & Makino, K. (2009), 'Conceptual design of a superconducting quadrupole with elliptical acceptance and tunable higher order multipoles', Int. J. Mod. Phys. A24, 923-940.”



Field Plots



Field plot on the transverse "X" axis vs "By"

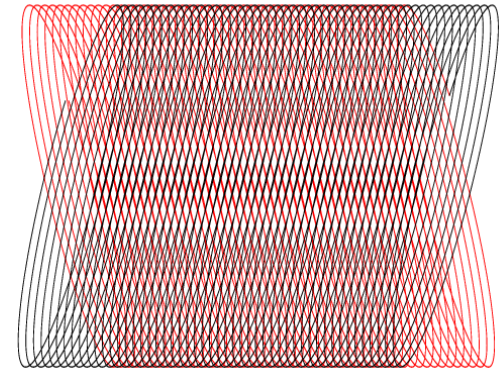


Field plot along "Z" axis vs "By" at x=15cm and y=0cm



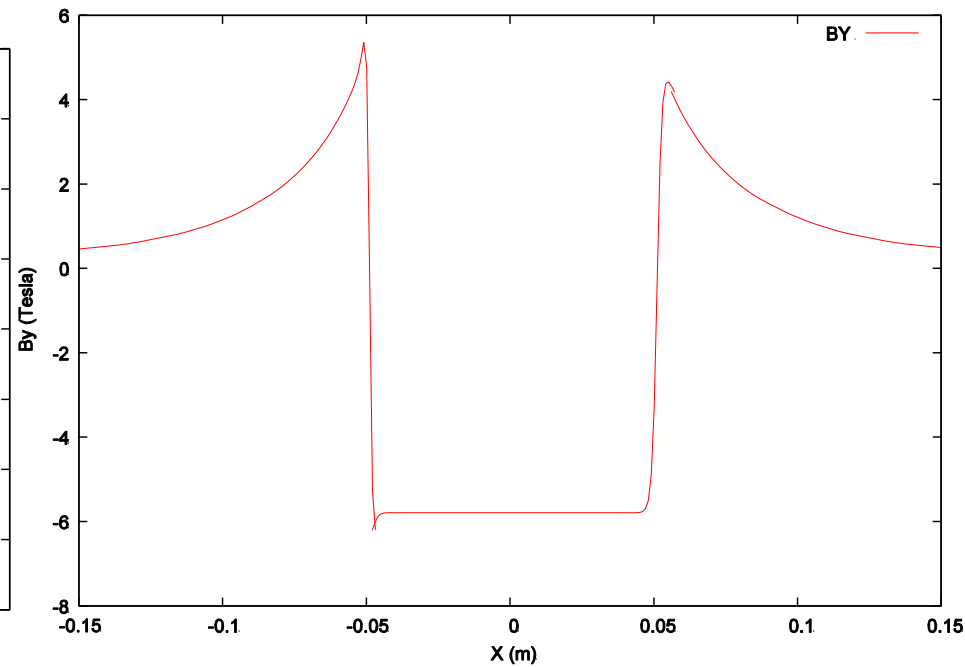
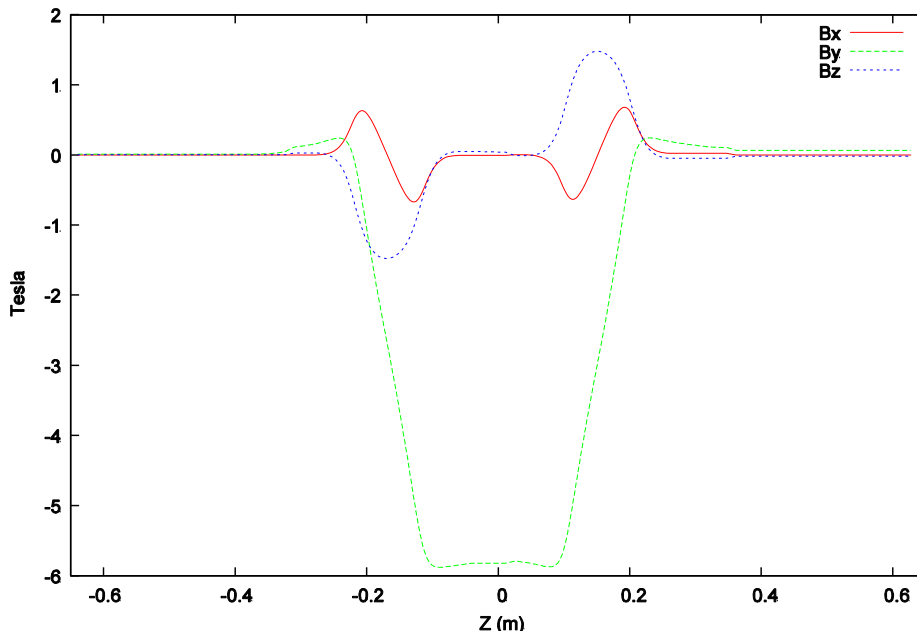
Double helix magnet design by Advanced Magnet Lab Inc.

$$z(\theta) = \frac{h\theta}{2\pi} + A_0 \left(\sin \theta + \sum_{n=2}^N \epsilon_n \sin(n\theta + \phi_n) \right)$$



Dipole Example

B vs z for X=0.025m and Y=0.025m

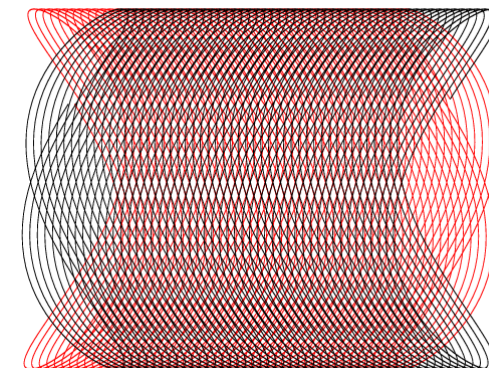


“Superconducting Double-Helix Accelerator Magnets, IEEE Proceedings of the 2003 Particle Accelerator Conference, 2003, Vol.3, pages 1996-1998. R.B. Meinke, M.J. Ball, C.L. Goodzeit”

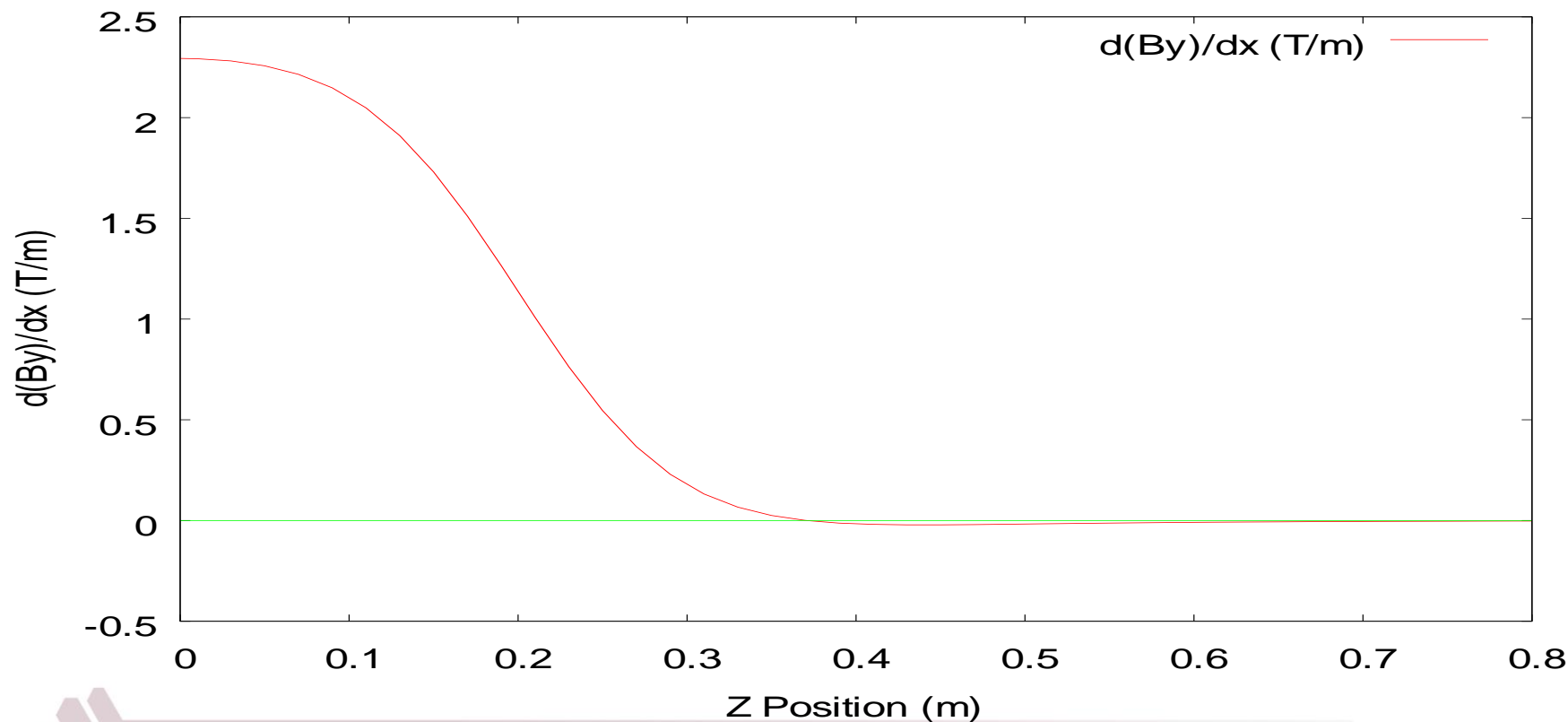


S3 Quadrupole Magnet: Double Helix Model

- Effective Length = 0.197 m
- Field Gradient Used = 2.29 T/m
- Has negative field gradient outside magnet



Double Helix Magnet: Field gradient along z



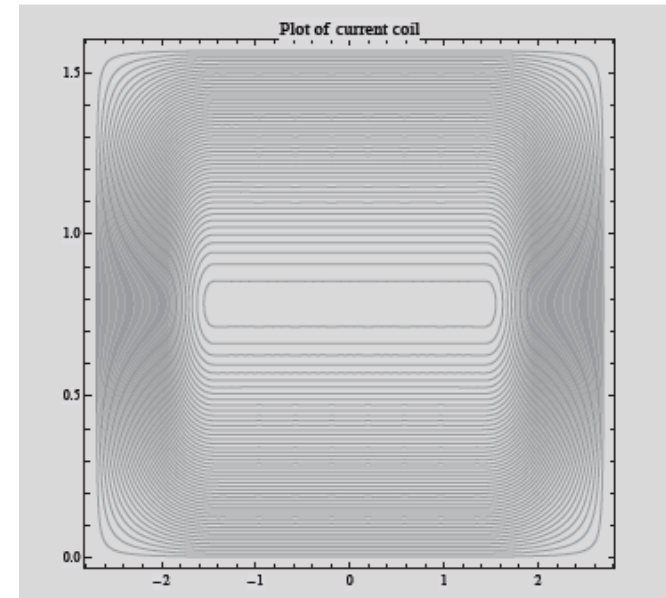
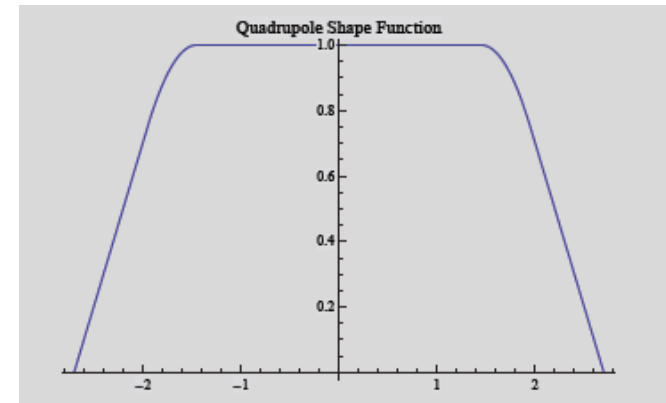
3-D cos mφ Magnets

- Proposed by P. L. Walstrom
- Based on using a shape function
- Produces pure cos mφ magnetic field in 3D

$$F(x) * \sin(m\phi) = (n - 1/2)/N$$

$$F(x) = \begin{pmatrix} kx & k \cdot 0.75x & k \\ 1.25kx^2 & k \cdot 1.25x & k \cdot 1.25 \\ 1 & k \cdot 1.25x & k \cdot 1.25 \\ 1.25kx^2 & k \cdot 0.75x & k \cdot 1.25 \\ kx & kx & k \cdot 0.75x \end{pmatrix}$$

Winding that produces pure quadrupole field
(m=2 and K=2.7, N=50)



“P. L. Walstrom, Soft-edged magnet models for higher-order beam-optics map codes, Nuclear Instruments and Methods in Physics Research Section A: Accelerators, Spectrometers, Detectors and Associated Equipment, Volume 519, Issues 1-2, Pages 216-221”

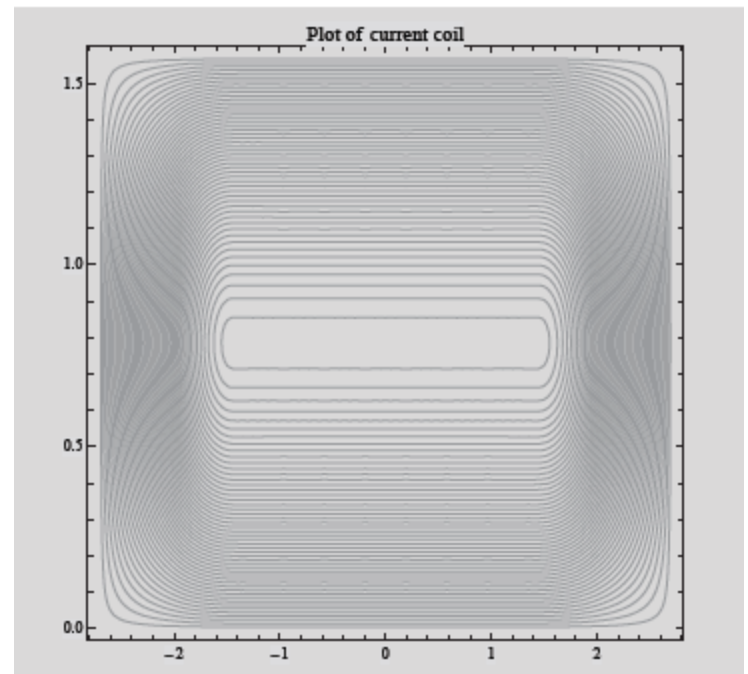
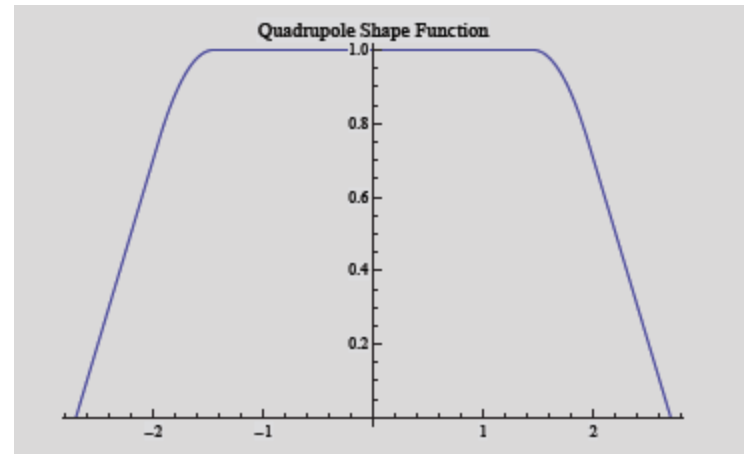
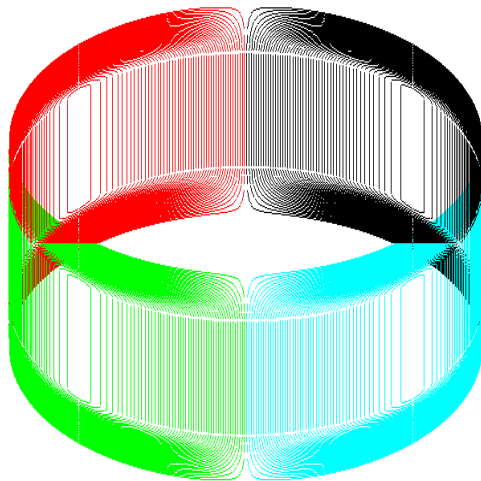


3D-Cos theta Quadrupole magnet

Winding Radius (m) = 0.17085

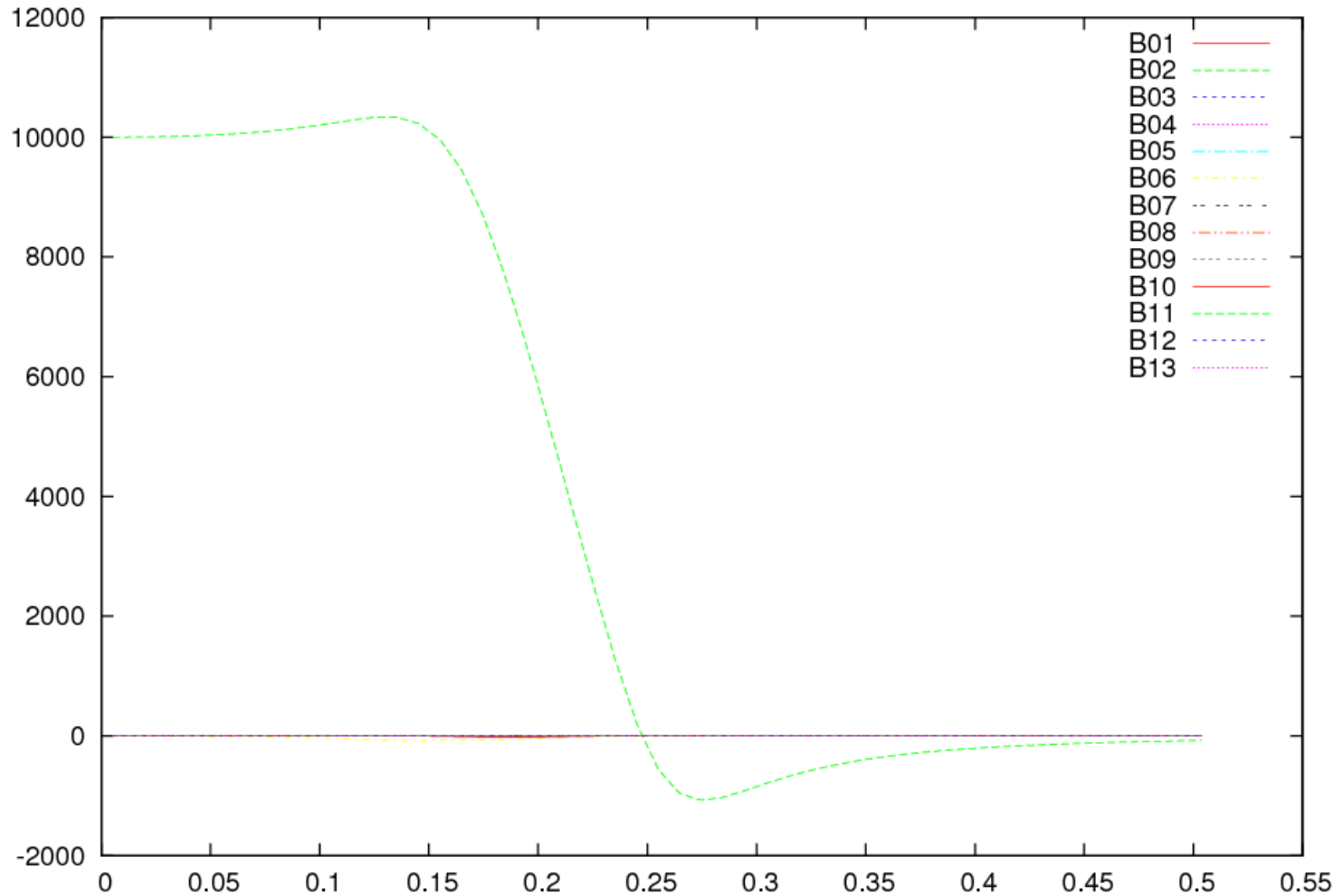
Total Number of turns = 50

Tip-to-tip total Coil Z Length (m) = 0.5

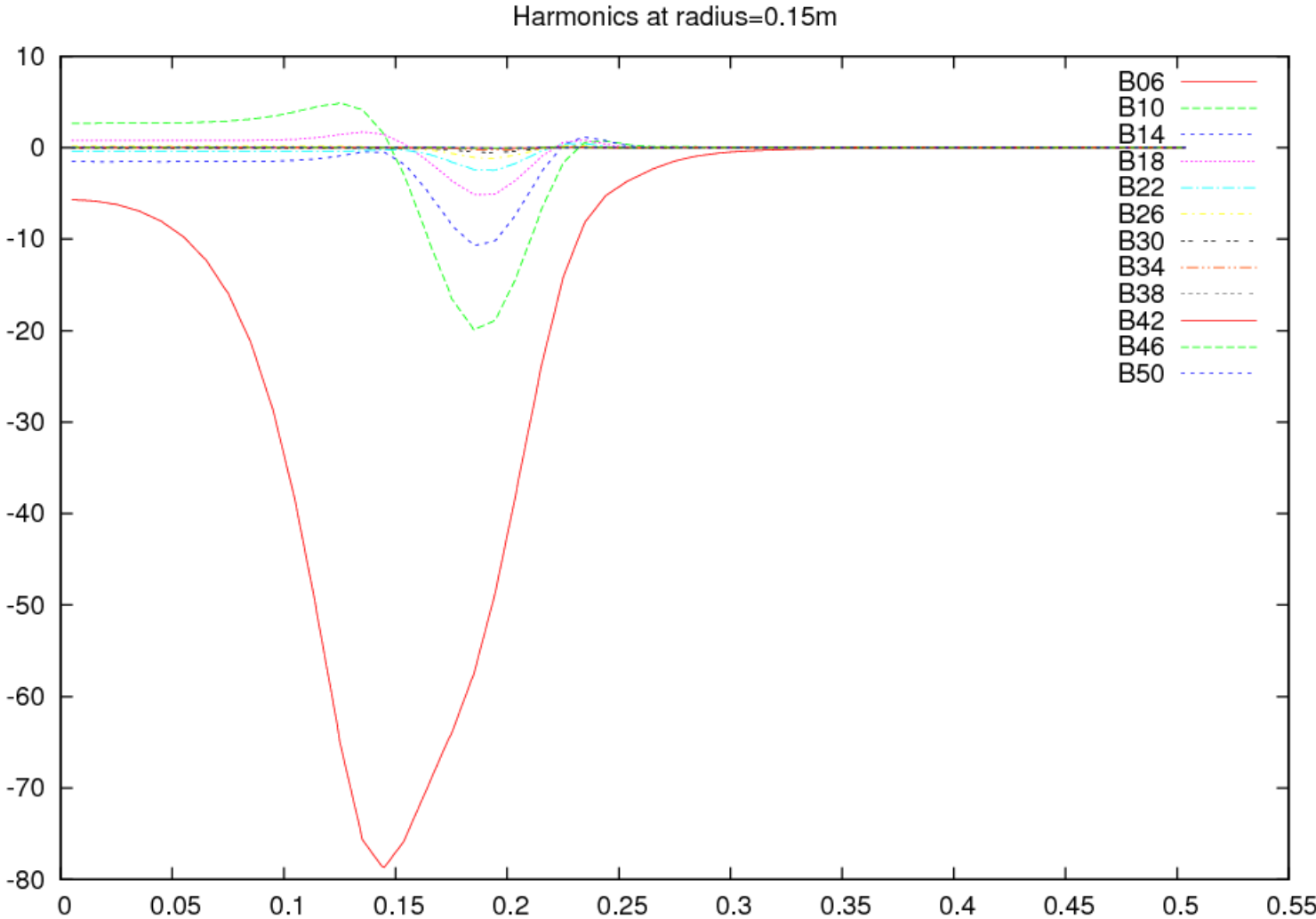


Harmonics for Quadrupole Magnet

Harmonics at radius=0.15m

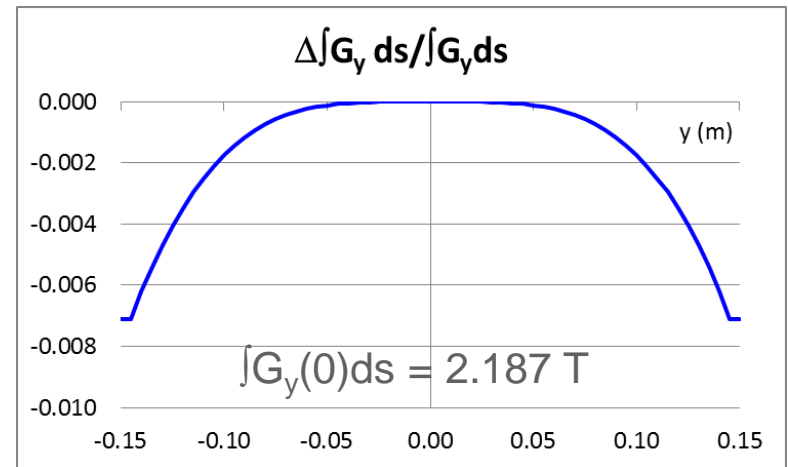
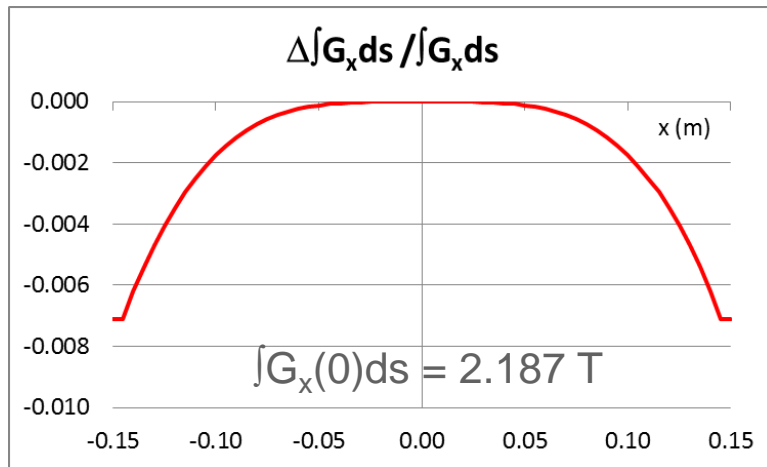


Allowed Higher order Harmonics for Quadrupole Magnet

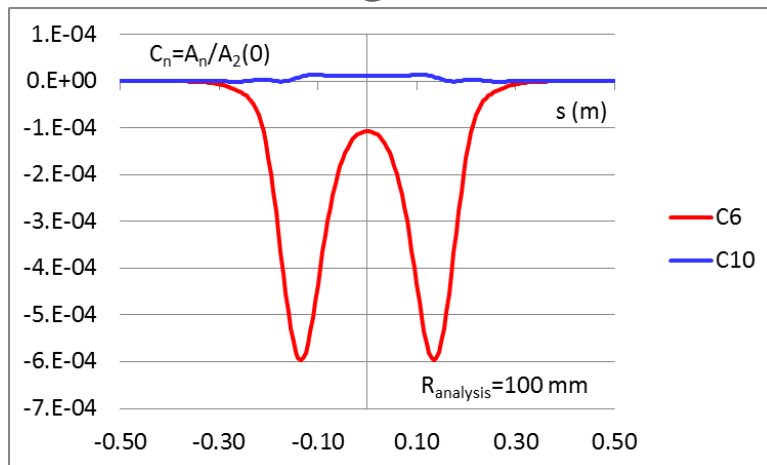


Quadrupole analysis

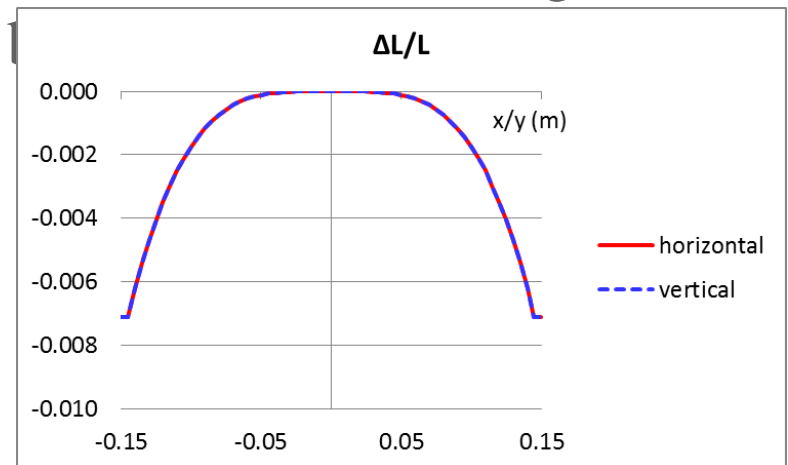
- J. Payet
- CEA/DSM/Irfu/SACM



Gradient integral (from -1500 to +1500 mm) homogeneities



Harmonic analysis



Magnetic length on the axis : **396** mm

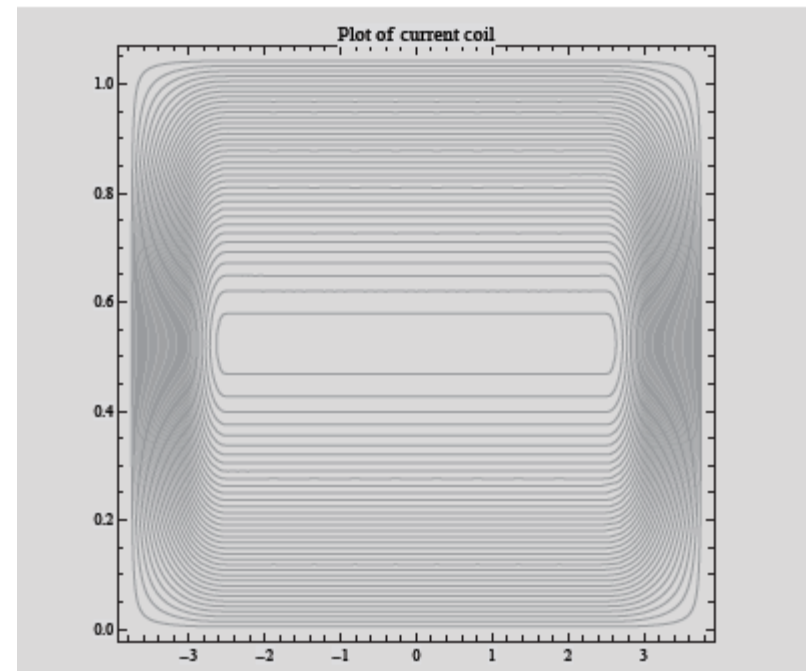
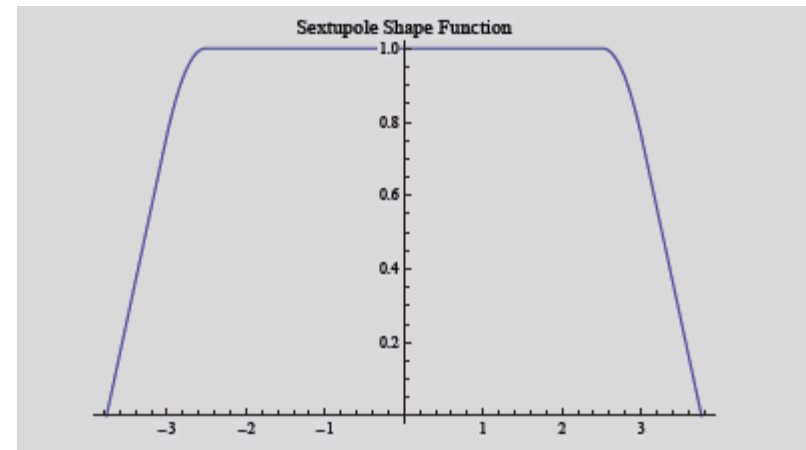
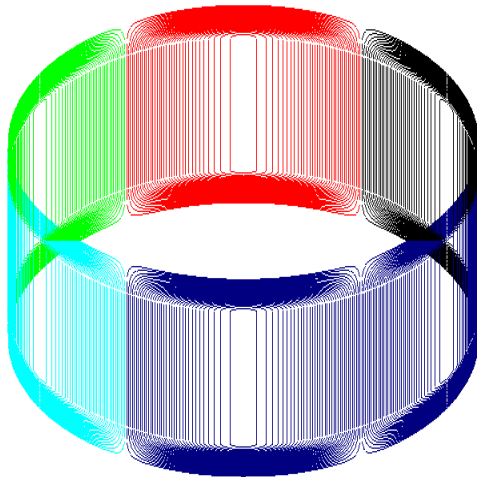


3D cos-theta Sextupole magnet

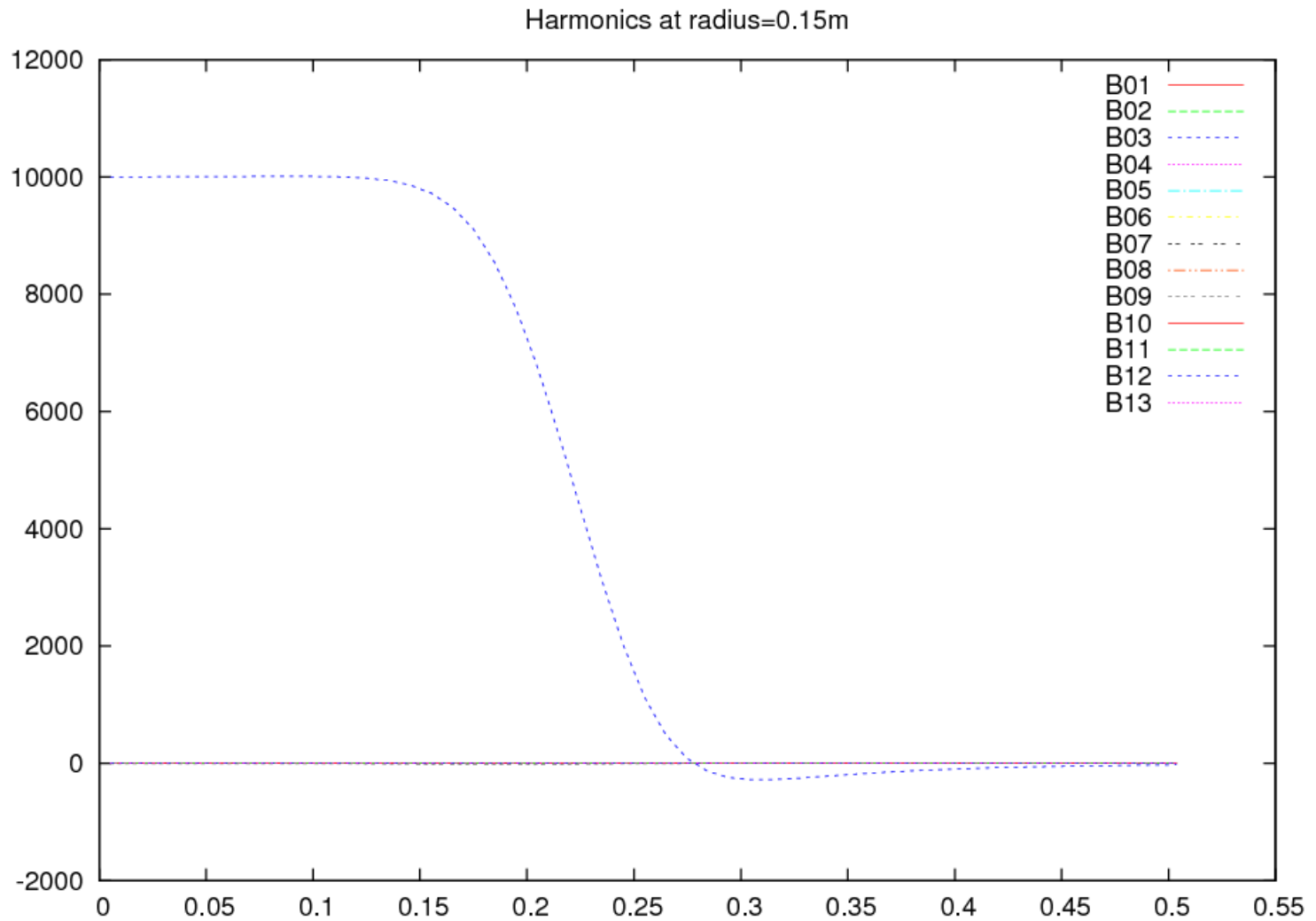
Winding Radius (m) = 0.20085

Total Number of turns = 36

Tip-to-tip total Coil Z Length (m) = 0.5

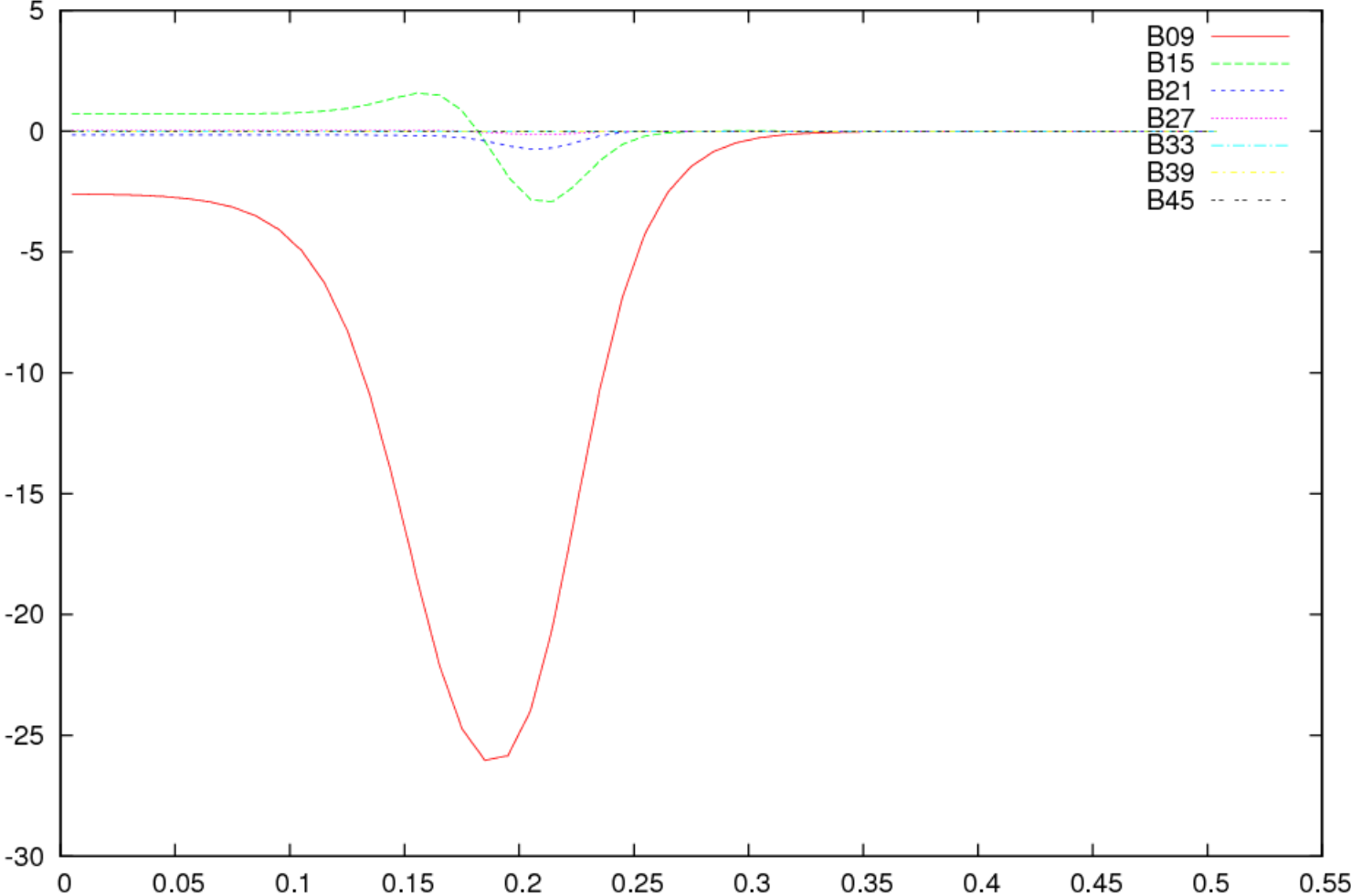


Harmonics for Sextupole Magnet

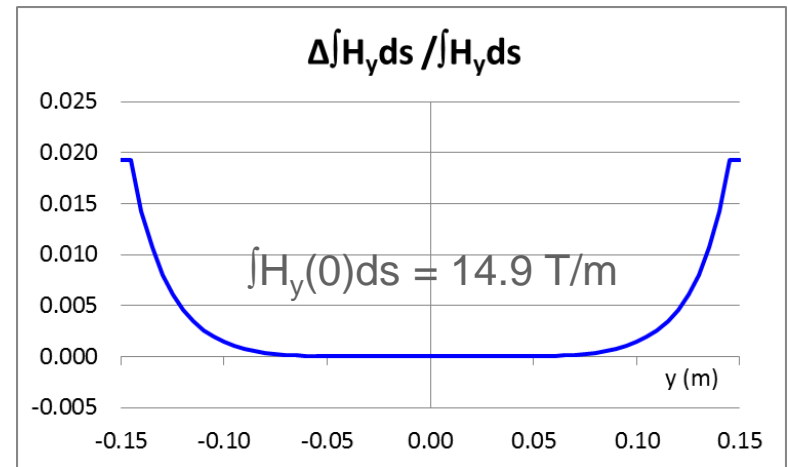
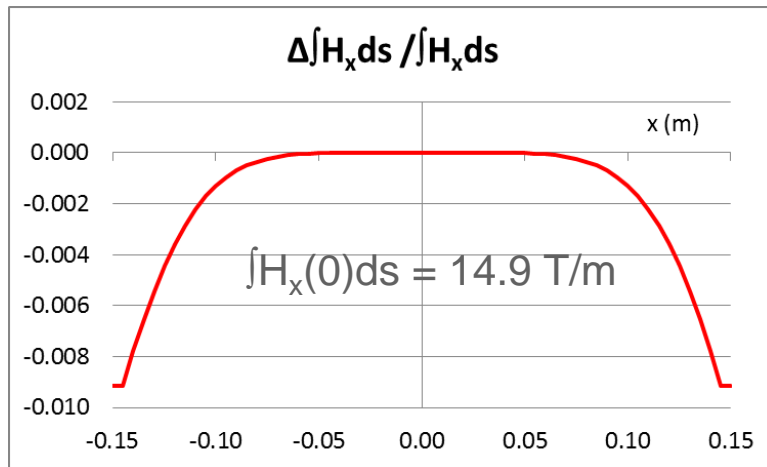


Allowed Higher order Harmonics for Sextupole Magnet

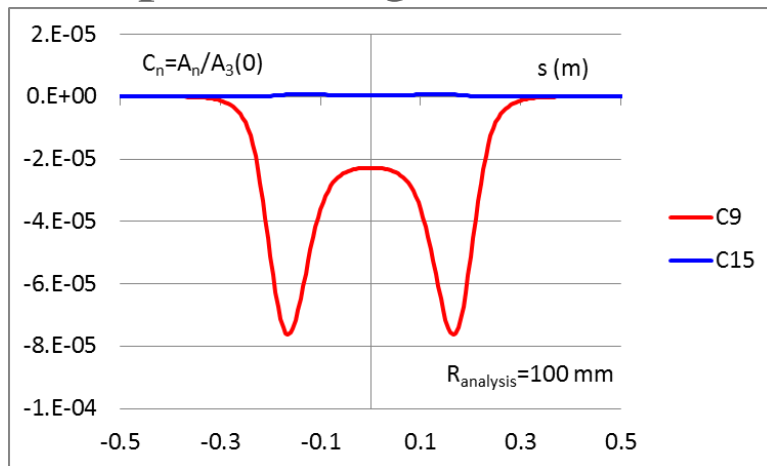
Harmonics at radius=0.15m



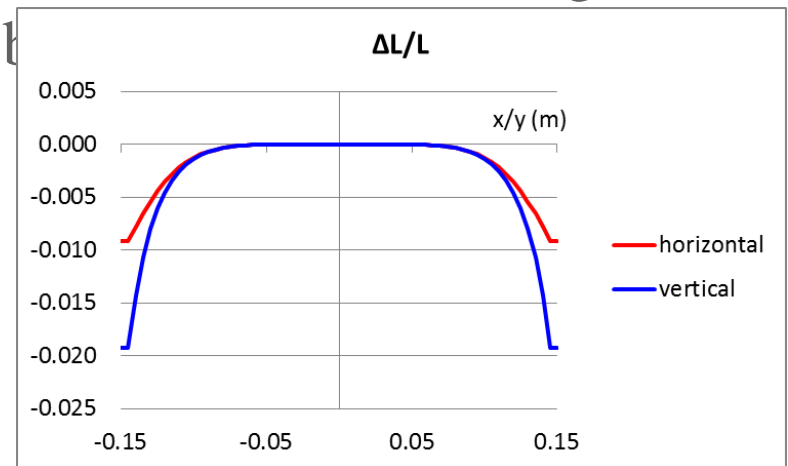
Sextupole analysis



Sextupolar integral (from -1500 to +1500 mm) homogeneities



Harmonic analysis



Magnetic length on the axis : **427 mm**

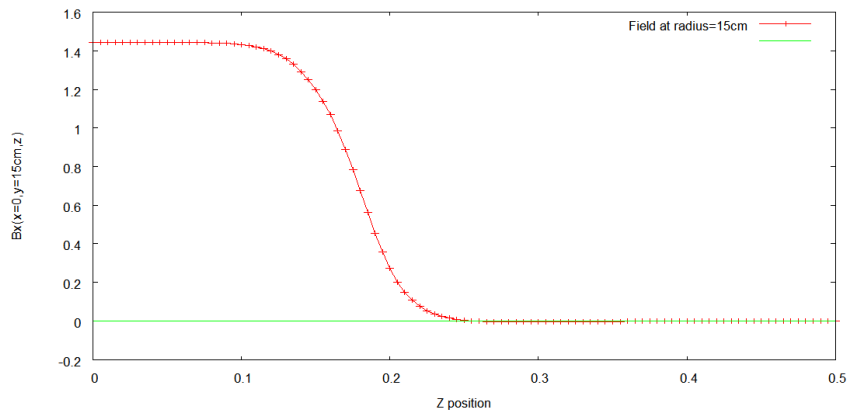
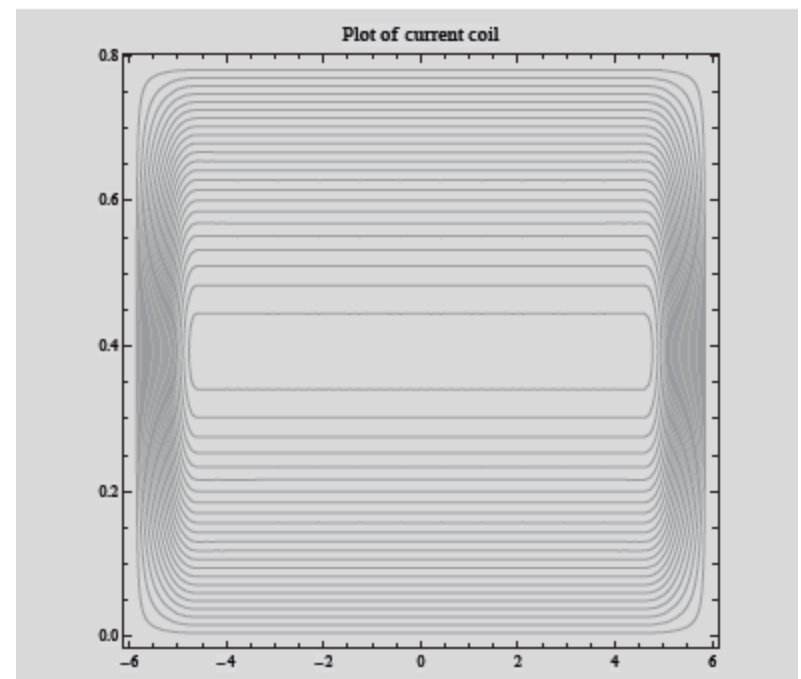
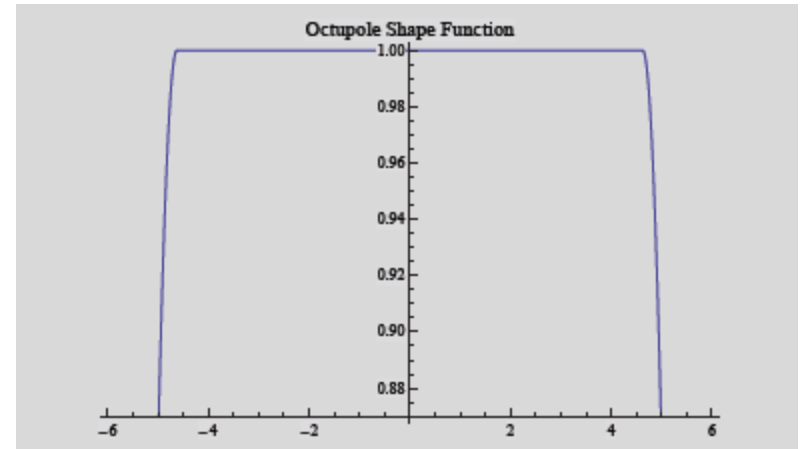
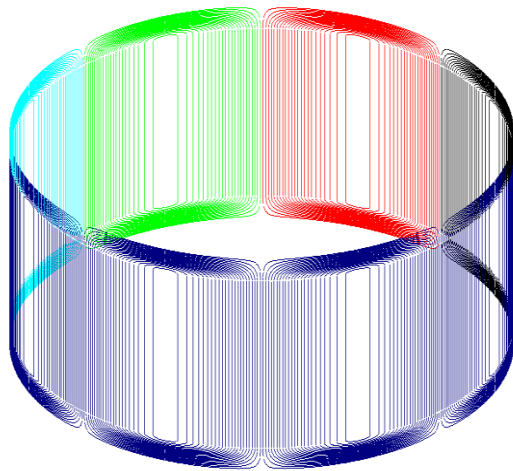


3D cost-theta octupole magnet

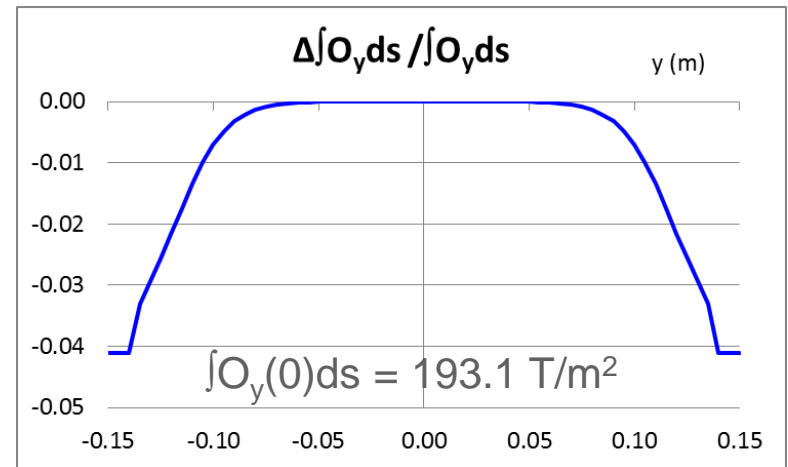
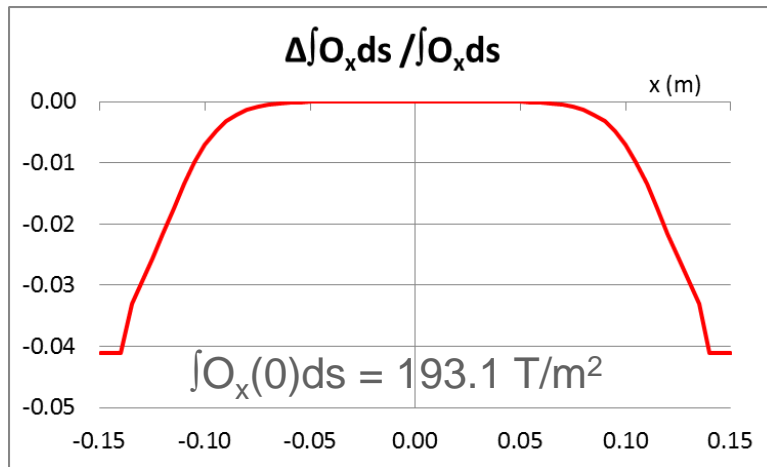
Winding Radius (m) = 0.1725

Total Number of turns = 23

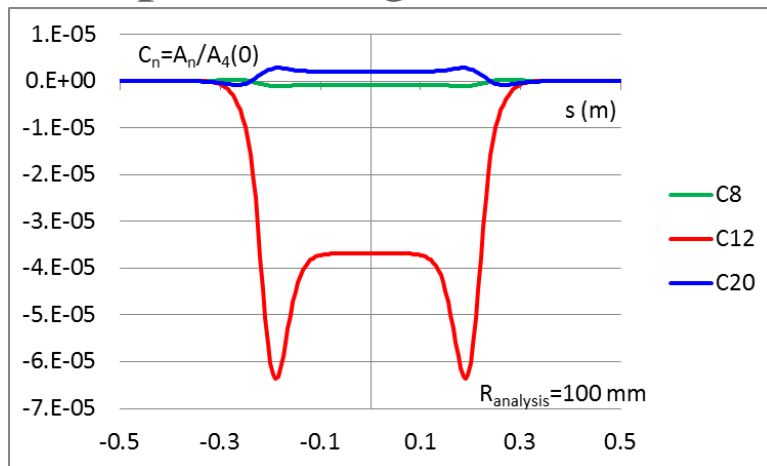
Tip-to-tip total Coil Z Length (m) = 0.5



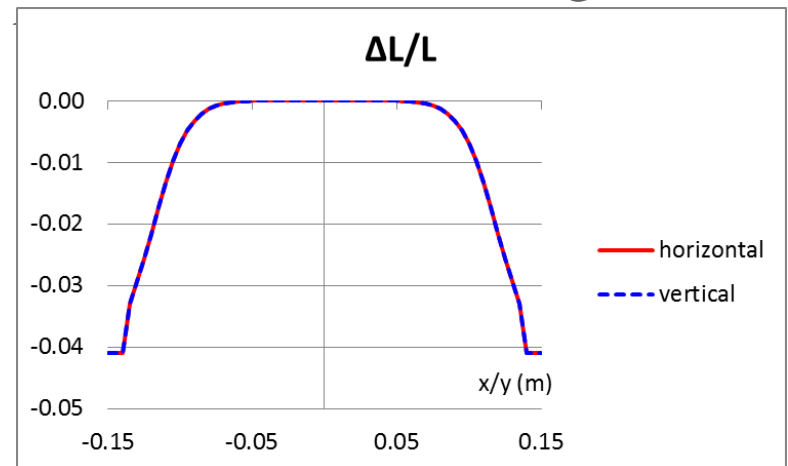
Octupole analysis



Octupolar integral (from -1500 to +1500 mm) homogeneities



Harmonic analysis



Magnetic length on the axis : **452** mm



Conclusion

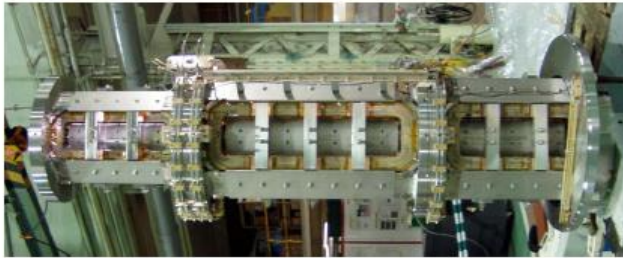
- Simulation studies were done to look at the feasibility of Superconducting option for S3 multipole magnets
- 3D cos-theta magnets were chosen as the basis for magnet bids
- New coil models have been implemented in COSY-Infinity code

Thank You!

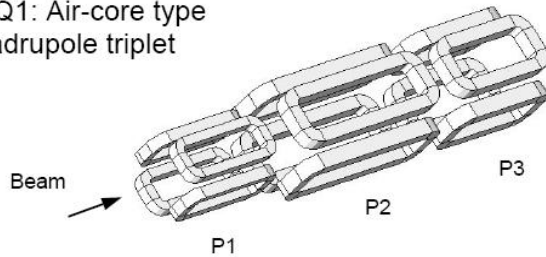


BigRIPS superconducting quad triplets

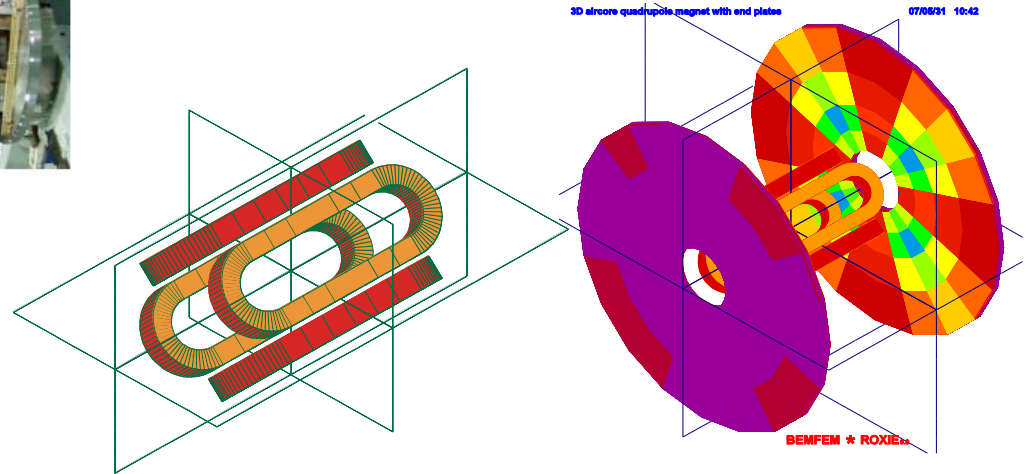
STQ1 cold mass



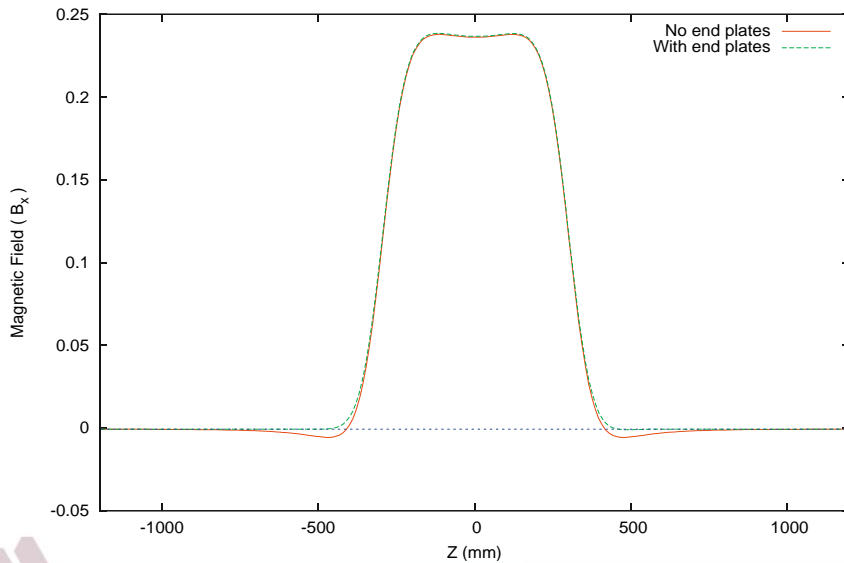
STQ1: Air-core type quadrupole triplet



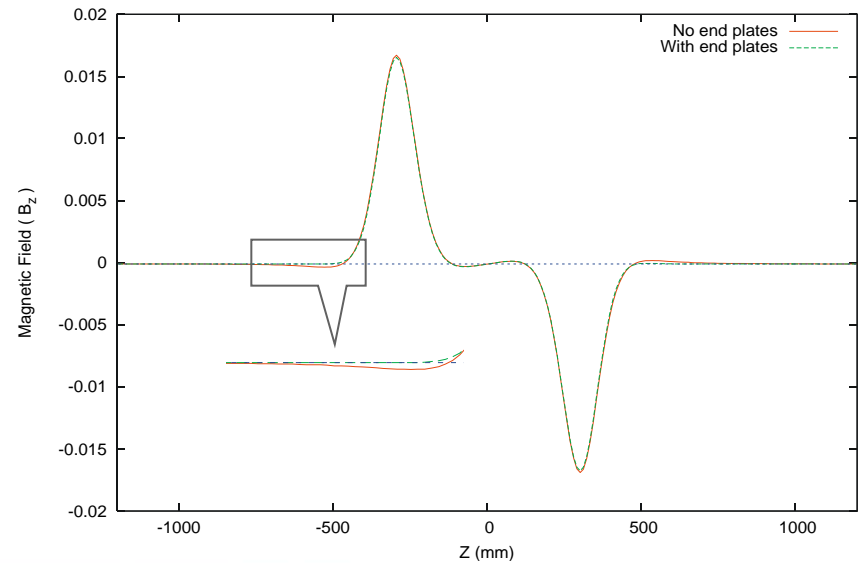
Roxie model to study the effect of end plates



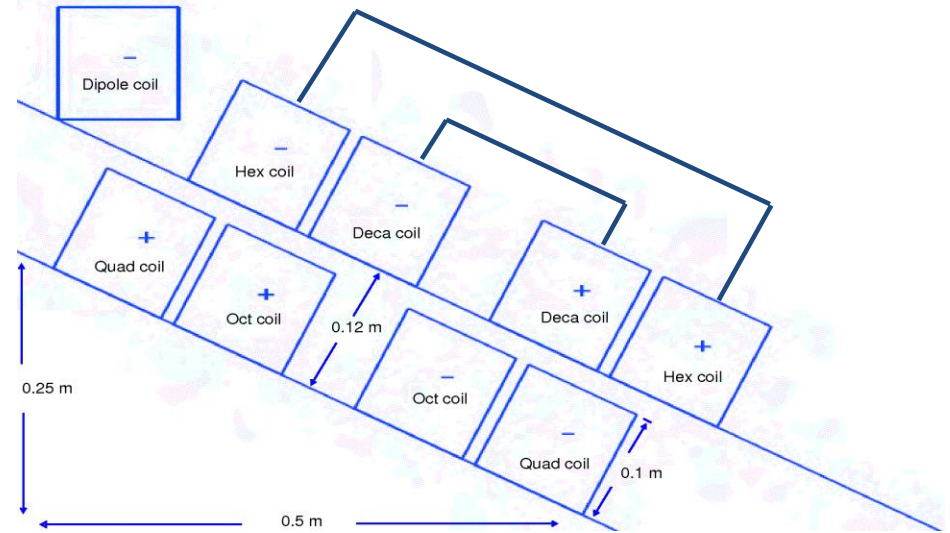
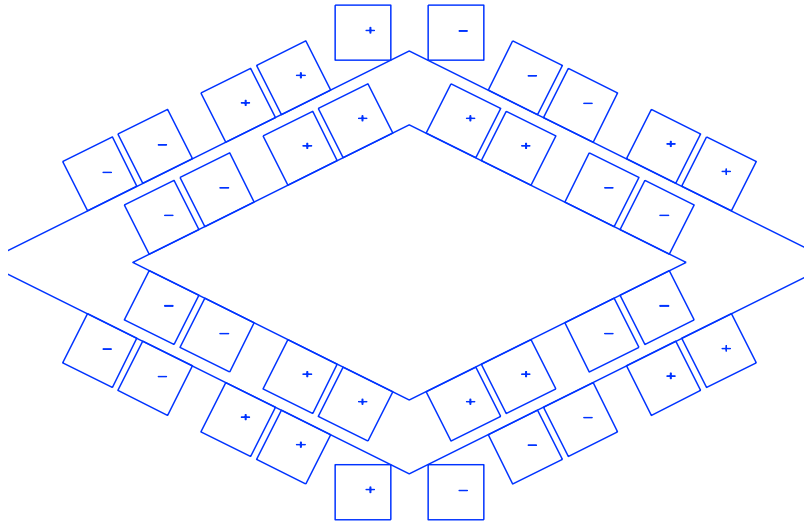
STQ1-P1: B_x VS z ($y=10\text{mm}$)



STQ1-P1: B_z VS z ($x=10\text{mm}, y=10\text{mm}$)



Design of quadrupole magnet with an elliptic cross section



- 18 superconducting racetrack coils ($\pm 10^8 \text{ A/m}^2$)
- Rhombic prism support structure (elliptic aperture 1:2)

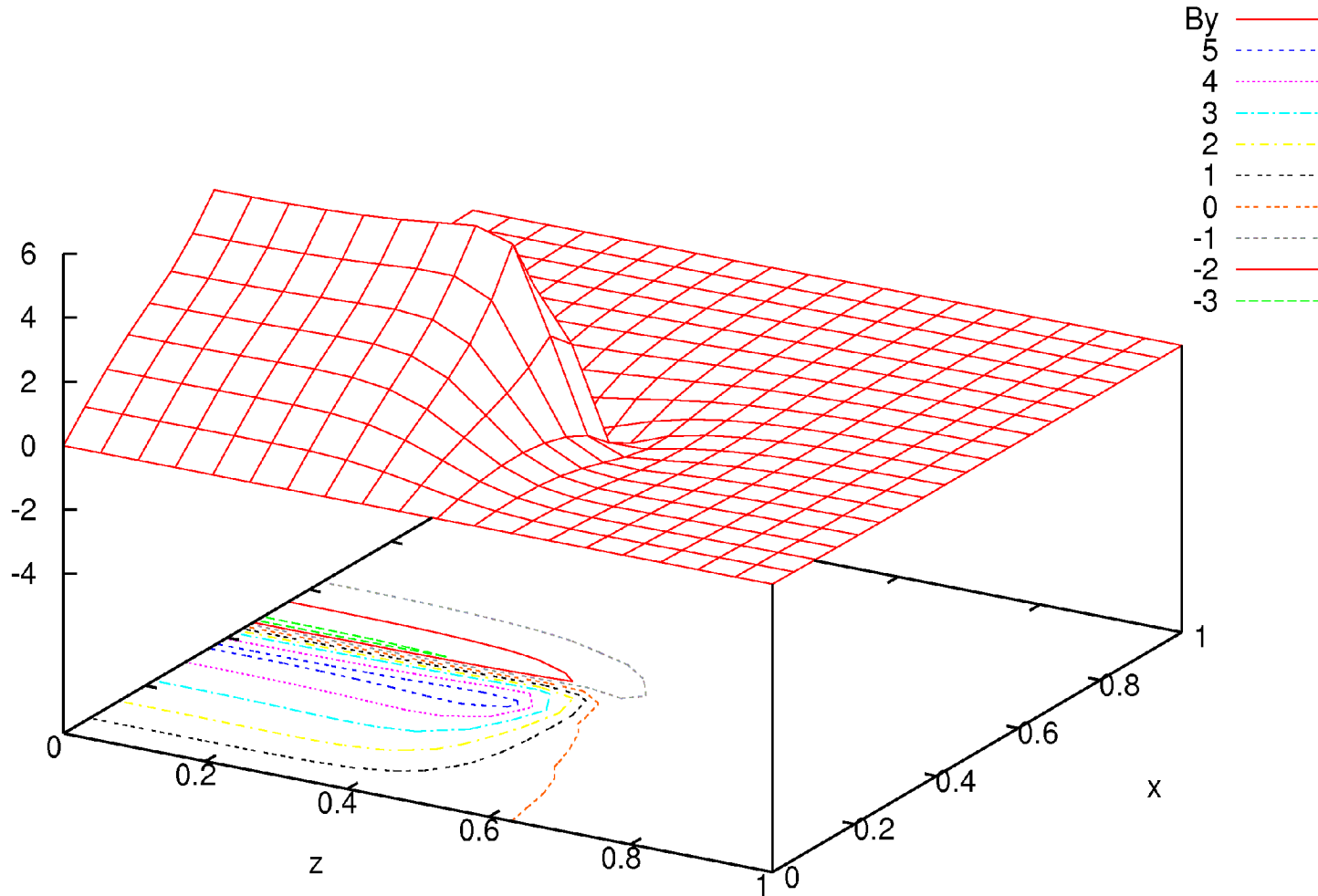
- "+" produces a positive multipole term
- Inner wires produce quadrupole and octupole fields
- Outer wires produce hexapole and decapole fields
- 2D case: two Infinitely long current wires
- 3D case: Current Coil

Using DA we can make the currents as parameters and find the functional dependence Of the multipole components on the coil currents.



3D Design: Fringe field

The plot of the magnetic field on the midplane, $y = 0$ m. Only the magnetic field in the first quadrant is shown.



The relationship between the currents and the principle multipole components can be given by a simple matrix

$$\begin{bmatrix} B_0^y \\ B_{(x)}^y \\ B_{(xx)}^y \\ B_{(xxx)}^y \\ B_{(xxxx)}^y \end{bmatrix} = \begin{bmatrix} 0 & 0 & -0.25 & -0.04 & +0.37 \\ +5.76 & +2.40 & 0 & 0 & 0 \\ 0 & 0 & -3.89 & -2.08 & -1.45 \\ -0.40 & +15.44 & 0 & 0 & 0 \\ 0 & 0 & +1.66 & -2.32 & +2.99 \end{bmatrix} \cdot \begin{bmatrix} QI \\ OI \\ HI \\ DI \\ I \end{bmatrix}$$

$$B_{(yy)}^y = -B_{(xx)}^y$$

$$B_{(xyy)}^y = -3B_{(xxx)}^y$$

$$-\frac{B_{(xxyy)}^y}{6} = B_{(yyyy)}^y = B_{(xxxx)}^y$$

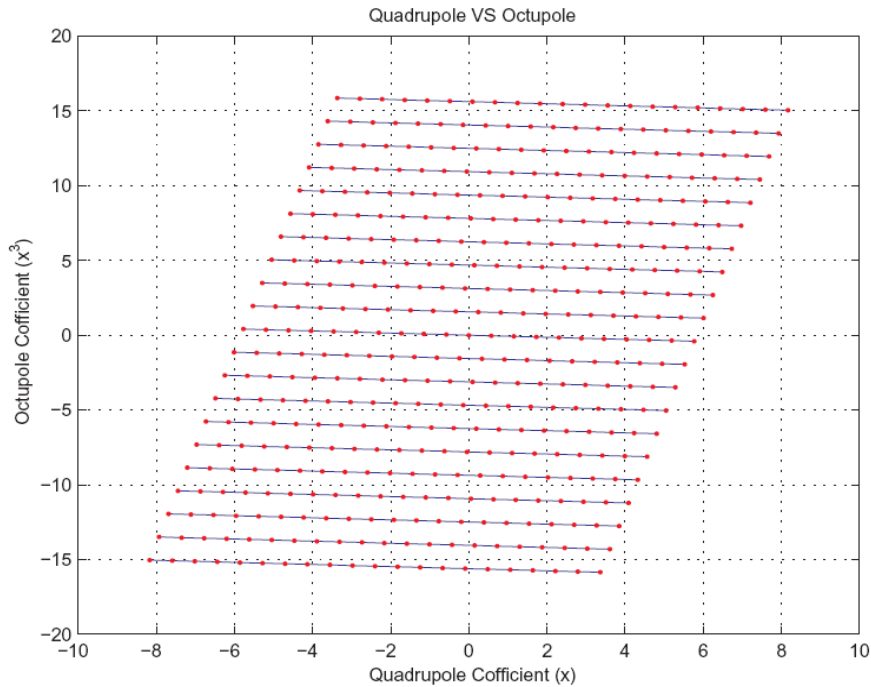
$$B_{(y)}^x = B_{(x)}^y$$

$$B_{(xy)}^x = 2B_{(xx)}^y$$

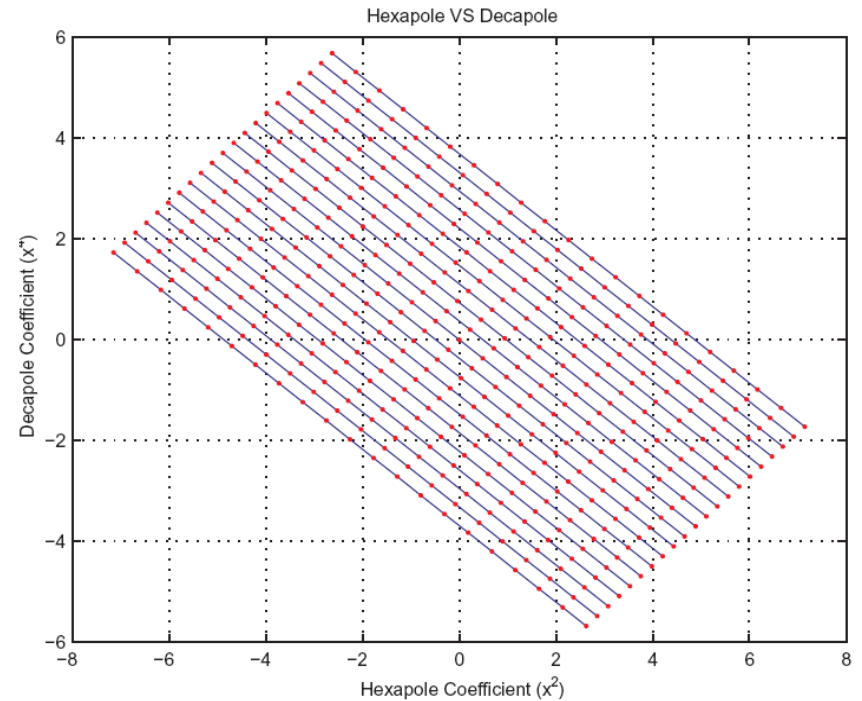
$$\frac{B_{(xxy)}^x}{3} = -B_{(yyy)}^x = B_{(xxx)}^y$$

$$B_{(xxx)}^x = -B_{(xyy)}^x = 4B_{(xxxx)}^y$$

Operational Plot



Quadrupole and the octupole terms

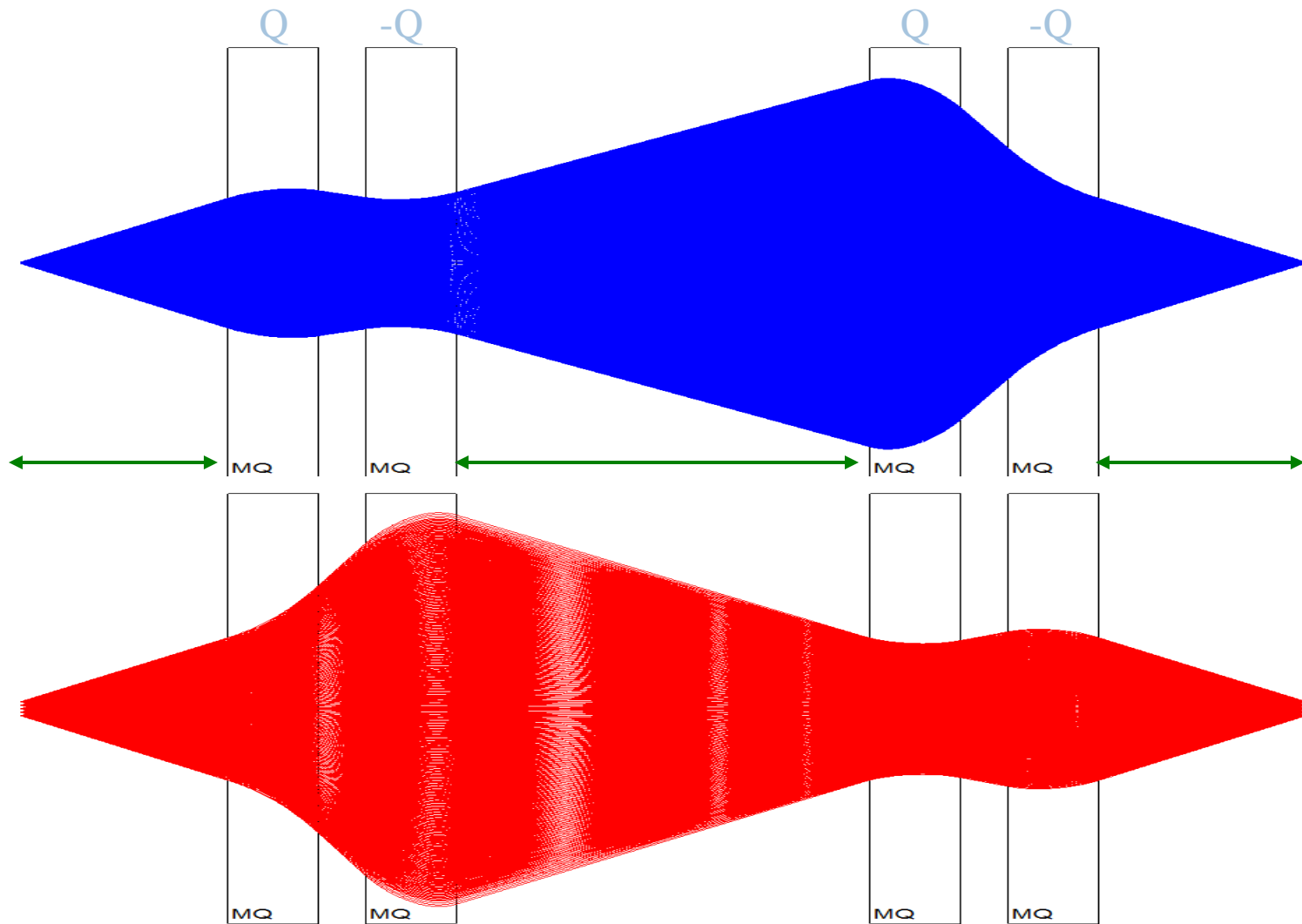


Hexapole and the Decapole terms

- The coefficients are computed at the horizontal half aperture
- The current density was varied between $\pm 10^8 \text{ A/m}^2$

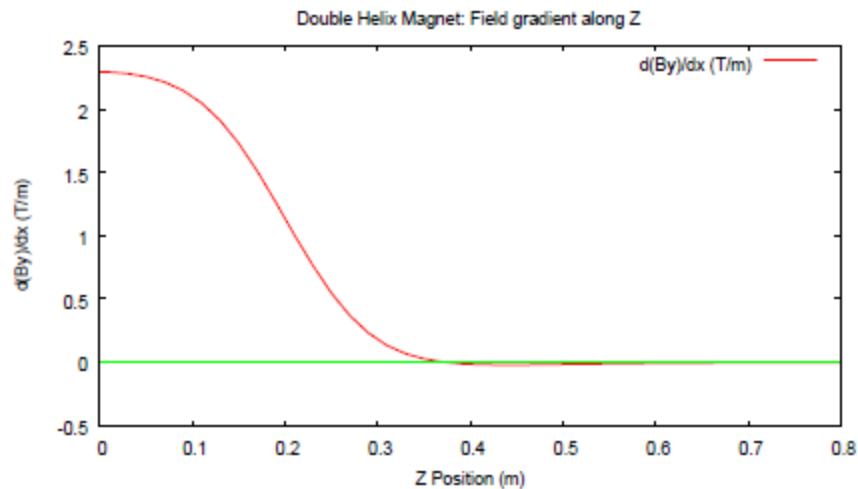
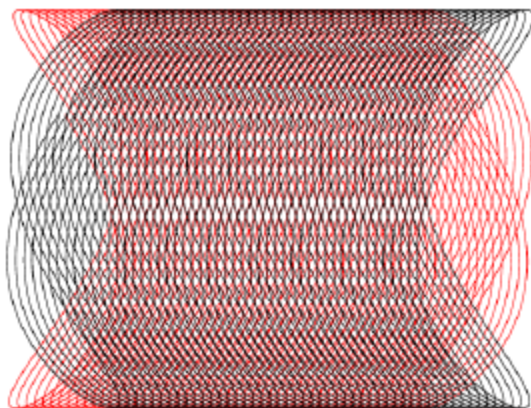
“Manikonda, S.; Nolen, J.; Berz, M. & Makino, K. (2009), 'Conceptual design of a superconducting quadrupole with elliptical acceptance and tunable higher order multipoles', Int. J. Mod. Phys. A24, 923-940.”

Double Doublet System



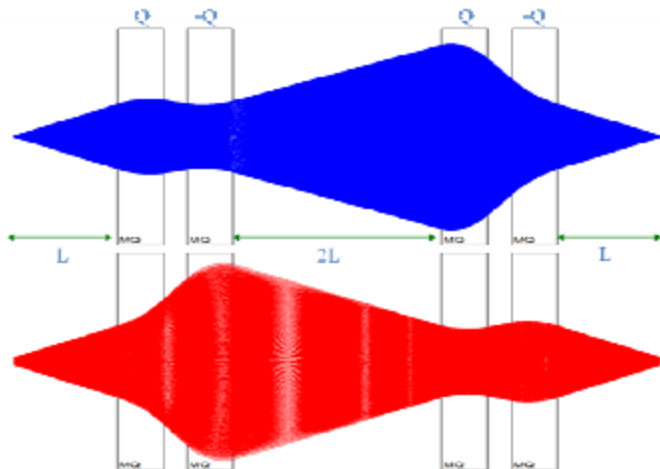
Negative Unit Transfer Map at First Order





| | | | | | |
|----------------|----------------|----------------|----------------|------------|--------|
| -1.542239 | -3.112883 | 0.000000 | 0.000000 | 0.000000 | 100000 |
| -0.4428486 | -1.542239 | 0.000000 | 0.000000 | 0.000000 | 010000 |
| 0.000000 | 0.000000 | 6.054183 | 7.132783 | 0.000000 | 001000 |
| 0.000000 | 0.000000 | 4.998544 | 6.054183 | 0.000000 | 000100 |
| 0.000000 | 0.000000 | 0.000000 | 0.000000 | 1.000000 | 000010 |
| 0.000000 | 0.000000 | 0.000000 | 0.000000 | 0.3749473 | 000001 |
| -0.2365723E-15 | -0.3202526E-15 | 0.000000 | 0.000000 | -1.002905 | 200000 |
| -0.3 | 0.0 | 0.0 | 0.0 | 0.0 | 000 |
| -0.4 | 0.0 | 0.0 | 0.0 | 0.0 | 000 |
| -0.7 | 0.0 | 0.0 | 0.0 | 0.0 | 000 |
| -0.1 | 0.0 | 0.0 | 0.0 | 0.0 | 000 |
| -0.2780024E-14 | -0.2882281E-14 | -0.8934582E-15 | -0.3533621E-14 | 0.000000 | 100100 |
| -0.3455668E-15 | 0.2033691E-14 | -0.3012454E-14 | -0.6370558E-14 | 0.000000 | 010100 |
| -0.2462000E-13 | -0.3510496E-13 | -0.8524214E-14 | -0.2201125E-13 | -13.66616 | 001100 |
| 0.7868733 | -0.7589147 | 0.000000 | 0.000000 | 0.000000 | 100001 |
| 0.8876815 | 0.7868733 | 0.000000 | 0.000000 | 0.000000 | 010001 |
| 0.000000 | 0.000000 | -3.317978 | -1.284662 | 0.000000 | 001001 |
| -0.9347198E-14 | -0.1377431E-13 | -0.4285249E-14 | -0.9906743E-14 | -6.032452 | 000200 |
| 0.000000 | 0.000000 | -4.732253 | -3.317978 | 0.000000 | 000101 |
| 0.000000 | 0.000000 | 0.000000 | 0.000000 | -0.2812382 | 000002 |
| | | | | 10.3 | Too |

Extracted Transfer Map



Comparison of double-helix with hardedge model



| Aberration Term | Double-Helix (m) | Hard-edge Model (m) |
|-----------------|------------------|---------------------|
| (x aδ) | 0.8193619E-02 | 0.8142576E-02 |
| (x aaa) | -0.8679288E-02 | -0.1505131E-02 |
| (x abb) | -0.8328710E-02 | -0.2521999E-03 |
| (x abbδ) | -0.1361716E-02 | small |
| (x aδδ) | small | -0.3458687E-03 |
| (x aa) | 0.1735195E-03 | small |
| (x bδδ) | -0.3518127E-03 | small |
| (x aaaδ) | 0.2515068E-03 | 0.1440338E-03 |
| (y bbb) | -0.2327891E-01 | -0.1505130E-02 |
| (y bbδ) | -0.8328712E-02 | small |
| (y ybb) | -0.4768876E-02 | small |
| (y bbbδ) | 0.1896777E-02 | small |
| (y bδ) | 0.8193619E-02 | 0.8142576E-02 |

